
Global Convergence and Induced Kernels of Gradient-Based Meta-Learning with Neural Nets

Haoxiang Wang, Ruoyu Sun, Bo Li
University of Illinois at Urbana-Champaign
{hwang264, ruoyus, lbo}@illinois.edu

Abstract

Gradient-based meta-learning (GBML) with deep neural nets (DNNs) has become a popular approach for few-shot learning. However, due to the non-convexity of DNNs and the complex bi-level optimization in GBML, the theoretical properties of GBML with DNNs remain largely unknown. In this paper, we first develop a novel theoretical analysis to answer the following questions: *Does GBML with DNNs have global convergence guarantees?* We provide a positive answer to this question by proving that GBML with over-parameterized DNNs is guaranteed to converge to *global optima* at a linear rate. The second question we aim to address is: *How does GBML achieve fast adaption to new tasks with experience on past similar tasks?* To answer it, we prove that GBML is equivalent to a *functional gradient descent* operation that explicitly propagates experience from the past tasks to new ones. Finally, inspired by our theoretical analysis, we develop a new kernel-based meta-learning approach. We show that the proposed approach outperforms GBML with standard DNNs on the Omniglot dataset when the number of past tasks for meta-training is *small*. The code is available at <https://github.com/AI-secure/Meta-Neural-Kernel>.

1 Introduction

Meta-learning has received much attention due to its applicability in few-shot learning, and meta reinforcement learning [41, 10]. The primary motivation for meta-learning is to fast learn a new task from a small amount of data, with prior experience on similar but different tasks. Gradient-based meta-learning (GBML) is a popular meta-learning approach, due to its simplicity and good performance in many meta-learning tasks [10]. Also, GBML represents a family of meta-learning methods that originate from the model-agnostic meta-learning (MAML) algorithm [11]. MAML formulates a bi-level optimization problem, where the inner-level objective represents the adaption to a given task, and the outer-level objective is the meta-training loss. Most GBML methods can be viewed as variants of MAML [34, 23, 13, 12, 38], and they are almost always applied together with deep neural networks (DNNs) in practice. Even though GBML with DNNs is empirically successful, this approach still lacks a thorough theoretical understanding.

Motivations

To theoretically understand why GBML works well in practice, we shall comprehend the *optimization* properties of GBML with DNNs. Several recent works theoretically analyze GBML in the case of *convex* objectives [12, 5, 23, 16, 44]. However, DNNs are always *non-convex*, so these works do not directly apply to GBML with DNNs. [9, 19, 38, 45] consider the non-convex setting, but they only provide convergence to *stationary points*. Since *stationary points* can have high training/test error, the convergence to them is not very satisfactory. Hence, a crucial question remains unknown for GBML optimization is: *Does GBML with DNNs have global convergence?*

The original intuition behind the design of GBML is that meta-learned DNN initializations can encode experience and error from past tasks to achieve fast adaption to new tasks, given past and new tasks are similar [11]. However, there is no rigorous theory to confirm this intuition. Hence, an important question that remains theoretically unclear is, *how does GBML achieve fast adaption to a new task with past experience on similar tasks?*

In practice, GBML usually uses a large number of past tasks for meta-training to achieve fast adaption to a task. However, real-world problems may only provide a few of them, and thus it is necessary to develop meta-learning approaches that work well in this *small-data* scenario.

Technical Challenges. In this paper, our primary goal is to provide theoretical guarantees on the optimization of GBML with DNNs. There exist two main challenges: (1) the non-convexity of DNNs, (2) the bi-level optimization of GBML that induces second-order gradient (i.e., Hessian) terms in gradient descent. In fact, both challenges are entangled together, which makes the theoretical analysis more challenging. To tackle them, we make use of the over-parameterization property of DNNs to ameliorate the non-convexity issue, and develop a novel analysis to handle the challenging second-order term of GBML that does not appear in classical supervised learning.

Main Contributions. In this paper, we first take the attempt to understand GBML with DNNs theoretically, and we make contributions in both theoretical and empirical aspects.

- **Global Convergence of GBML with wide DNNs:** We prove that with over-parameterized DNNs (i.e., DNNs with a large number of neurons in each layer), GBML is guaranteed to converge to global optima at a linear rate. The key to our proof is to develop bounds on the gradient of the GBML objective, which contains Hessian terms, and then analyze the optimization trajectory of DNN parameters trained under GBML. To the best of our knowledge, it is the first global convergence guarantee for GBML parameterized with neural networks¹.
- **A Theoretical Understanding on How GBML Works:** Based on the global convergence analysis, we theoretically demonstrate that with over-parameterized DNNs, GBML is equivalent to a *functional gradient descent* that explicitly propagates the prior knowledge about past tasks to new tasks. This explains how GBML achieves fast adaption to new tasks and verifies the intuition behind the design of GBML theoretically.
- **An Meta-Learning Method with Great Performance in the Small-Data Scenario:** Extending the theoretical analysis to extremely over-parameterized DNNs (i.e., DNNs with an infinite number of neurons in each layer), we prove GBML is equivalent to a *kernel* regression with a new class of kernels, which we name as Meta Neural Kernels (MNKs). We implement this kernel-based meta-learning method and show it outperforms GBML with standard DNNs on the Omniglot dataset in small-data cases, i.e., the data for meta-training is of a small size, which is a realistic scenario for many real-world tasks. In addition, we believe this equivalence between GBML and kernel methods can provide a novel perspective for researchers to analyze GBML.

2 Preliminaries

In this section, we start by introducing the typical setup for few-shot learning. Then we review MAML, the seed of most GBML methods. Notations defined in this section will be adopted in the entire paper.

2.1 Few-Shot Learning

Consider a few-shot learning problem with a set of *training tasks* that contains N supervised-learning tasks $\{\mathcal{T}_i\}_{i=1}^N$. Each task is represented as $\mathcal{T}_i = (X_i, Y_i, X'_i, Y'_i) \in \mathbb{R}^{n \times d} \times \mathbb{R}^{n \times k} \times \mathbb{R}^{m \times d} \times \mathbb{R}^{m \times k}$, where (X'_i, Y'_i) represents m support samples (i.e. training samples of \mathcal{T}_i) and corresponding labels in this task, while (X_i, Y_i) represents n query samples (i.e. test samples of \mathcal{T}_i) and corresponding labels. For convenience, we denote $\mathcal{X} = (X_i)_{i=1}^N$, $\mathcal{Y} = (Y_i)_{i=1}^N$, $\mathcal{X}' = (X'_i)_{i=1}^N$, and $\mathcal{Y}' = (Y'_i)_{i=1}^N$.

In few-shot learning, $\{\mathcal{T}_i\}_{i=1}^N$ are training tasks for learners to train on (i.e., for meta-training). In the inference stage, an arbitrary test task $\mathcal{T} = (X, Y, X', Y')$ is picked, and the support samples and labels (X', Y') are given to the trained learner as input, then the learner is asked to output its prediction on the labels of the query samples X from \mathcal{T} .

¹See also the concurrent work of [43].

2.2 Gradient-Based Meta-Learning

GBML is equipped with parametric models, which are almost always neural networks in practice. Consider a parametric model f with parameters θ such that $f_\theta : \mathbb{R}^d \mapsto \mathbb{R}^k$, and its output on arbitrary sample $x \in \mathbb{R}^d$ is $f_\theta(x)$. Suppose an arbitrary task is given as $\mathcal{T} = (X, Y, X', Y')$. In GBML, it is helpful to define the *meta-output*, $F : (X', Y') \mapsto f_{\theta'}$, a mapping depending on support samples and labels such that $F_\theta(\cdot, X', Y') = f_{\theta'}(\cdot)$, where θ' is the *adapted parameters* depending on θ and (X', Y') . Specifically, we define F as the vectorized output of the model f with adapted parameters,

$$F_\theta(X, X', Y') = f_{\theta'}(X) = \text{vec}([f_{\theta'}(x)]_{x \in X}) \in \mathbb{R}^{nk} \quad (1)$$

where the adapted parameters θ' is obtained as follows: use θ as the initial parameter and update it by τ steps of gradient descent on support samples and labels (X', Y') , with learning rate λ and loss function ℓ . Mathematically,

$$\theta = \theta_0, \quad \theta' = \theta_\tau, \quad \text{and} \quad \theta_{i+1} = \theta_i - \lambda \nabla_{\theta_i} \ell(f_{\theta_i}(X'), Y') \quad \forall i = 0, \dots, \tau - 1, \quad (2)$$

With the square loss function $\ell(\hat{y}, y) = \frac{1}{2} \|\hat{y} - y\|_2^2$, the training objective of MAML² is

$$\mathcal{L}(\theta) = \sum_{i=1}^N \ell(F_\theta(X_i, X'_i, Y'_i), y_i) = \frac{1}{2} \sum_{i=1}^N \|F_\theta(X_i, X'_i, Y'_i) - Y_i\|_2^2 = \frac{1}{2} \|F_\theta(\mathcal{X}, \mathcal{X}', \mathcal{Y}') - \mathcal{Y}\|_2^2 \quad (3)$$

where $F_\theta(\mathcal{X}, \mathcal{X}', \mathcal{Y}') \equiv (F_\theta(X_i, X'_i, Y'_i))_{i=1}^N = \text{vec}([F_\theta(X_i, X'_i, Y'_i)]_{i \in [N]})$ is the meta-outputs on all training tasks.

Remarks on second-order gradients. It is well known that running gradient descent on GBML objectives induces second-order gradient terms, which make theoretical analyses difficult. Below, we briefly show how this issue occurs. For simplicity, let us consider the case of only one step of adaption, i.e., $\tau = 1$. Denote $\theta'_i = \theta - \lambda \nabla_{\theta} \ell(f_\theta(X'_i), Y'_i)$. Then, the gradient of $\mathcal{L}(\theta)$ can be obtained by the chain rule,

$$\nabla_{\theta} \mathcal{L}(\theta) = \sum_{i=1}^N \nabla_{\theta} \ell(f_{\theta'_i}(X_i), Y_i) = \sum_{i=1}^N [I - \lambda \nabla_{\theta}^2 f_\theta(X_i)] (f_{\theta'_i}(X'_i) - Y'_i) \quad (4)$$

where I is the identity matrix and $\nabla_{\theta}^2 f_\theta(X_i)$ is a second-order gradient (i.e., Hessian). Since gradient descent is a first-order optimization method, its theoretical analyses generally do not involve second-order gradients. Hence, the second-order gradients complicate the optimization analysis of GBML. Furthermore, in the case of GBML parameterized by neural networks, the Hessian terms become more difficult to handle because of the non-convexity of neural networks.

3 Global Convergence of Gradient-Based Meta-Learning with Over-parameterized Deep Neural Networks

In this section, we will show for sufficiently over-parameterized deep neural networks, GBML is guaranteed to convergence to global optima under gradient descent at a linear rate. Besides, we will demonstrate that this convergence analysis can give rise to an analytical expression of GBML output.

Consider a neural network f_θ with L hidden layers, where $\theta \in \mathbb{R}^D$ is a vector containing all the parameters of the network. For $i \in [L]$, we use l_i to denote the width of the i -th hidden layer. In this paper, we consider all hidden layers have the same width l for simplicity, i.e., $l_1 = l_2 = \dots = l_L = l$. For notational convenience, we denote the Jacobian of the meta-output on training data as $J(\theta) = \nabla_{\theta} F_\theta(\mathcal{X}, \mathcal{X}', \mathcal{Y}')$, and define a kernel function as $\hat{\Phi}_\theta(\cdot, \star) := \frac{1}{l} \nabla_{\theta} F_\theta(\cdot) \nabla_{\theta} F_\theta(\star)^\top$. Also, we define η as the learning rate for gradient descent on the GBML objective, (3); for any diagonalizable matrix M , we use $\sigma_{\min}(M)$ and $\sigma_{\max}(M)$ to denote the least and largest eigenvalues of M . These notations will be adopted in the entire paper.

²Although we only demonstrate the MAML objective in (3), slight modifications to (3) can convert it to many other GBML objectives, including 1st-order MAML [11, 34], Adaptive GBML [23], WrapGrad [14] and Meta-Curvature [35], etc.

To prove the global convergence of GBML with DNNs, we need to first prove the Jacobian of the meta-output, J , changes locally in a small region under perturbations on network parameters, θ . Because of the non-convexity of DNNs and the second-order gradients induced by the bi-level optimization of GBML, it is non-trivial to obtain such a result. However, we manage to prove this by developing a novel analysis to bound the change of Jacobian under parameter perturbations, shown below as a lemma, with detailed proof in Appendix B.

Lemma 1 (Local Lipschitzness of Jacobian). *Suppose³ $\tau = \mathcal{O}(\frac{1}{\lambda})$, then there exists $K > 0$ such that: $\forall C > 0$, the following inequalities hold true with high probability over random initialization,*

$$\forall \theta, \bar{\theta} \in B(\theta_0, Cl^{-\frac{1}{2}}), \begin{cases} \frac{1}{\sqrt{l}} \|J(\theta) - J(\bar{\theta})\|_F & \leq K \|\theta - \bar{\theta}\|_2 \\ \frac{1}{\sqrt{l}} \|J(\theta)\|_F & \leq K \end{cases} \quad (5)$$

where B is a neighborhood defined as

$$B(\theta_0, R) := \{\theta : \|\theta - \theta_0\|_2 < R\}. \quad (6)$$

Suppose the neural net is sufficiently over-parameterized, i.e., the width of hidden layers, l , is large enough. Then, we can prove GBML with this neural net is guaranteed to converge to global optima (i.e., the training loss converges to zero) at a linear rate, under several mild assumptions. The detailed setup and proof can be found in Appendix B. We provide a simplified theorem with a proof sketch below.

Theorem 2 (Global Convergence). *Define $\Phi = \lim_{l \rightarrow \infty} \frac{1}{l} J(\theta_0) J(\theta_0)^T$. For any $\delta_0 > 0$, $\eta_0 < \frac{2}{\sigma_{\max}(\Phi) + \sigma_{\min}(\Phi)}$, and $\tau = \mathcal{O}(\frac{1}{\lambda})$ there exist $R_0 > 0$, $\Lambda \in \mathbb{N}$, $K > 1$, and $\lambda_0 > 0$, such that: for width $l \geq \Lambda$, running gradient descent with learning rates $\eta = \frac{\eta_0}{l}$ and $\lambda < \frac{\lambda_0}{l}$ over random initialization, the following upper bound on the training loss holds true with probability at least $(1 - \delta_0)$:*

$$\mathcal{L}(\theta_t) = \frac{1}{2} \|F_{\theta_t}(\mathcal{X}, \mathcal{X}', \mathcal{Y}') - \mathcal{Y}\|_2^2 \leq \left(1 - \frac{\eta_0 \sigma_{\min}(\Phi)}{3}\right)^{2t} \frac{R_0^2}{2}. \quad (7)$$

Proof Sketch. First, we consider the Jacobian of the meta-output, J , and prove a lemma showing J has bounded norm. Then we prove another lemma showing Φ is a deterministic matrix over random initialization of θ_0 . By these lemmas and Lemma 1, we analyze the optimization trajectory of the neural net parameters, and prove the parameters move locally during optimization, and the training loss exponentially decays as the number of optimization steps increases, indicating the training loss converges to zero at a linear rate, shown as (7). \square

With this global convergence theorem, we can derive an analytical expression for GBML output at any training time, shown below as a corollary, with proof in Appendix B.

Corollary 2.1 (GBML Output). *In the setting of Theorem 2, the training dynamics of the GBML can be described by a differential equation*

$$\frac{dF_t(\mathcal{X}, \mathcal{X}', \mathcal{Y}')}{dt} = -\eta \hat{\Phi}_0(F_t(\mathcal{X}, \mathcal{X}', \mathcal{Y}') - \mathcal{Y})$$

where we denote $F_t \equiv F_{\theta_t}$ and $\hat{\Phi}_0 \equiv \hat{\Phi}_{\theta_0}((\mathcal{X}, \mathcal{X}', \mathcal{Y}'), (\mathcal{X}, \mathcal{X}', \mathcal{Y}'))$ for convenience.

Solving this differential equation, we obtain the meta-output of GBML on training tasks at any training time as

$$F_t(\mathcal{X}, \mathcal{X}', \mathcal{Y}') = (I - e^{-\eta \hat{\Phi}_0 t}) \mathcal{Y} + e^{-\eta \hat{\Phi}_0 t} F_0(\mathcal{X}, \mathcal{X}', \mathcal{Y}'). \quad (8)$$

Similarly, on arbitrary test task $\mathcal{T} = (X, Y, X', Y')$, the meta-output of GBML is

$$F_t(X, X', Y') = F_0(X, X', Y') + \hat{\Phi}_0(X, X', Y') T_{\hat{\Phi}_0}^\eta(t) (\mathcal{Y} - F_0(\mathcal{X}, \mathcal{X}', \mathcal{Y}')) \quad (9)$$

where $\hat{\Phi}_0(\cdot) \equiv \hat{\Phi}_{\theta_0}(\cdot, (\mathcal{X}, \mathcal{X}', \mathcal{Y}'))$ and $T_{\hat{\Phi}_0}^\eta(t) = \hat{\Phi}_0^{-1} (I - e^{-\eta \hat{\Phi}_0 t})$ are shorthand notations.

³This assumption is realistic in practice. For example, the official implementation of MAML [11] for few-shot classification benchmarks adopts (i) $\tau = 1$, $\lambda = 0.4$ and (ii) $\tau = 5$, $\lambda = 0.1$, which both satisfy our assumption.

Remarks. This corollary implies for a sufficiently over-parameterized neural network, the training of GBML is *determined* by the *parameter initialization*, θ_0 . Given access to θ_0 , we can compute the functions $\hat{\Phi}_0$ and F_0 , and then the trained GBML output can be obtained by simple calculations, without the need for running gradient descent on θ_0 . This nice property enables us to perform deeper analysis on GBML with DNNs in the following sections.

4 Gradient-Based Meta-Learning as Functional Gradient Descent

The empirical success of GBML methods is mainly due to their ability to learn good DNN initializations for adaption on new tasks [10]. However, it is not theoretically clear why these learned initializations are effective. This section provides some theoretical insight on this problem by demonstrating equivalence between GBML with DNNs and a functional gradient descent operation. A toy example of GBML is shown in Sec. 4.1 to further illustrate this equivalence to functional gradient descent.

Note that the GBML output (9) can be rewritten as

$$\underbrace{F_t(X, X', Y')}_{\text{Meta Learner}} = \underbrace{F_0(X, X', Y')}_{\text{Base Learner}} - \underbrace{\underbrace{\hat{\Phi}_0(X, X', Y') T_{\hat{\Phi}_0}^\eta(t)}_{\text{Projection}} \underbrace{\nabla_{F_0} \mathcal{L}[F_0]}_{\text{Functional Gradient}}}_{\text{Projected Functional Gradient}} \quad (10)$$

where \mathcal{L} is a loss *functional* (i.e., function with functions as input) such that for any function h ,

$$\mathcal{L}[h] = \frac{1}{2} \|h(\mathcal{X}, \mathcal{X}', \mathcal{Y}') - \mathcal{Y}\|_2^2,$$

with the corresponding *functional gradient* on the function h as

$$\nabla_h \mathcal{L}[h] = \nabla_{h(\mathcal{X}, \mathcal{X}', \mathcal{Y}')} \mathcal{L}[h] = h(\mathcal{X}, \mathcal{X}', \mathcal{Y}') - \mathcal{Y}.$$

Obviously, (10) can be seen as a *projected functional gradient descent* operation on F_0 , with learning rate equal to 1 and $\hat{\Phi}_0(X, X') T_{\hat{\Phi}_0}^\eta(t)$ as the *projection*.

The function F_0 can be viewed as the output of a purely *supervised learning* model that has no thing to do with meta-learning, since $F_0(X, X', Y')$ is just the prediction on X by a randomly initialized DNN trained under gradient descent on the training set (X', Y') . More specifically, from (1) we can see that $F_0(X, X', Y') = F_{\theta_0}(X, X', Y') = f_{\theta'_0}(X)$, where θ'_0 is the adapted parameters upon random initialized parameters θ_0 trained under τ steps of gradient descent on (X', Y') . Therefore, F_0 can be viewed as a supervised learning model trained on the dataset (X', Y') .

In other words, F_0 can be viewed as a *base learner* (i.e., a supervised learning model), and the goal of GBML is to train a *meta-learner* (i.e., a meta-learning model), F_t , to improve the performance of the base learner on test tasks, by utilizing the prior knowledge on training tasks.

Hence, for over-parameterized DNNs, the effect of GBML is equivalent to the second term in (10), a *projected functional gradient* that can be also viewed as an *error correction* term to the base learner F_0 , which propagates prior knowledge on training tasks $(\mathcal{X}, \mathcal{Y}, \mathcal{X}', \mathcal{Y}')$ to the base model on the test task $\mathcal{T} = (X, Y, X', Y')$ to reduce its test error.

4.1 An Example for Illustration

To illustrate the equivalence between GBML and functional gradient descent derived in (10), we present a simple but insightful example of few-shot learning, *1-d few-shot regression with quadratic objective functions*, in which all samples and labels are scalars.

A key assumption in meta-learning is the *task similarity*: training and test tasks are *similar* in some way. In this example, we consider a class of quadratic objective functions that enjoy task similarity. Specifically, for arbitrary task $\mathcal{T} = (X, Y, X', Y')$, the relation between its samples and labels is determined by a unique scalar variable, $\alpha \sim \text{Unif}(0, 1)$, such that

$$Y = \alpha X^2 \text{ and } Y' = \alpha X'^2.$$

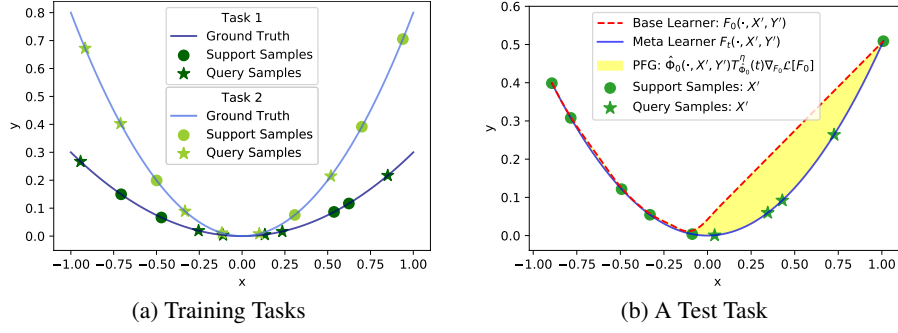


Figure 1: Illustration of the example in Sec. 4.1. (a) shows two training tasks, their support and query samples, and the corresponding ground-truth objective functions. (b) first shows a test task with support and query samples. Besides, it demonstrates several terms defined in (10): the predictions of the meta learner and the base learner, and the projected functional gradient (PFG) term, which is equal to the difference between the first two terms.

Each training task in $\{\mathcal{T}_i\}_{i=1}^N$ has its own α , so does each test task. Then, it is natural to expect that GBML can comprehend the quadratic nature of objective functions from training tasks, then utilize this prior knowledge to achieve fast adaption to any test task with only a few samples.

Suppose all samples are drawn uniformly from $[0, 1]$. Then, the training tasks are distributed, as shown in Fig. 1(a), and a test task is shown in Fig. 1(b). The meta-learner trained over these training tasks, F_t , is able to predict well on the query samples of this test task, even with only a few support samples that are distributed imbalanced, since it knows the objective functions are all quadratic. However, a base learner without any prior knowledge, F_0 , cannot give accurate predictions on these query samples, even though it shares the same DNN structure and parameter initialization with the meta learner, since it does not know the quadratic nature of the ground-truth objective functions.

Eq. (10) provides a mathematical explanation to the relation between the base learner and the meta learner, for GBML with over-parameterized DNNs. The difference between their predictions on query samples is exactly a *projected functional gradient* term. From this perspective, the meta-learner is obtained by directly performing a functional gradient descent operation on the function of the base learner.

Remarks. This functional gradient descent result provides a novel *function-space* perspective for theoretical studies on GBML, instead of the common *parameter-space* view. Since DNNs are highly non-convex, it is hard to theoretically understand the fast adaption ability of GBML by analyses on the parameter space. However, in the function space, GBML can be expressed in a simpler form, as shown by (10). Hence, we believe the insightful *function-space* perspective can lead to a new direction to study the fast adaption achieved by GBML.

5 Gradient-Based Meta-Learning as Kernel Regression

In this section, we will show for extremely over-parameterized DNNs, GBML is equivalent to a special kernel regression with a new class of kernels, which we name as Meta Neural Kernels. The proof of the following theorem can be found in Appendix. E.

Theorem 3 (GBML as Kernel Regression). *Suppose learning rates η and λ are infinitesimal. As the network width l approaches infinity, with high probability over random initialization of the neural net, the GBML output, (9), converges to a special kernel regression,*

$$F_t(X, X', Y') = G_{\Theta}^{\tau}(X, X', Y') + \Phi((X, X'), (\mathcal{X}, \mathcal{X}')) T_{\Phi}^{\eta}(t) (\mathcal{Y} - G_{\Theta}^{\tau}(\mathcal{X}, \mathcal{X}', \mathcal{Y}')) \quad (11)$$

where G is a function defined below, Θ is the neural tangent kernel (NTK) function from [17] that can be analytically calculated without constructing any neural net, and Φ is a new kernel, which name as Meta Neural Kernel (MNK). The expression for G is

$$G_{\Theta}^{\tau}(X, X', Y') = \Theta(X, X') \tilde{T}_{\Theta}^{\lambda}(X', \tau) Y'. \quad (12)$$

where $\tilde{T}_\Theta^\lambda(\cdot, \tau) := \Theta(\cdot, \cdot)^{-1}(I - e^{-\lambda\Theta(\cdot, \cdot)\tau})$. Besides, $G_\Theta^\tau(\mathcal{X}, \mathcal{X}', \mathcal{Y}) = (G_\Theta^\tau(X_i, X'_i, Y'_i))_{i=1}^N$.

The MNK is defined as $\Phi \equiv \Phi((\mathcal{X}, \mathcal{X}'), (\mathcal{X}, \mathcal{X}')) \in \mathbb{R}^{knN \times knN}$, which is a block matrix that consists of $N \times N$ blocks of size $kn \times kn$. For $i, j \in [N]$, the (i, j) -th block of Φ is

$$[\Phi]_{ij} = \phi((X_i, X'_i), (X_j, X'_j)) \in \mathbb{R}^{kn \times kn}, \quad (13)$$

where $\phi : (\mathbb{R}^{n \times k} \times \mathbb{R}^{m \times k}) \times (\mathbb{R}^{n \times k} \times \mathbb{R}^{m \times k}) \rightarrow \mathbb{R}^{nk \times nk}$ is a kernel function defined as

$$\begin{aligned} \phi((\cdot, \star), (\bullet, \star)) &= \Theta(\cdot, \bullet) + \Theta(\cdot, \star)\tilde{T}_\Theta^\lambda(\star, \tau)\Theta(\star, \star)\tilde{T}_\Theta^\lambda(\star, \tau)^\top\Theta(\star, \bullet) \\ &\quad - \Theta(\cdot, \star)\tilde{T}_\Theta^\lambda(\star, \tau)\Theta(\star, \bullet) - \Theta(\cdot, \star)\tilde{T}_\Theta^\lambda(\star, \tau)^\top\Theta(\star, \bullet). \end{aligned} \quad (14)$$

The $\Phi((X, X'), (\mathcal{X}, \mathcal{X}')) \in \mathbb{R}^{kn \times knN}$ in (11) is also a block matrix, which consists of $1 \times N$ blocks of size $kn \times kn$, with the $(1, j)$ -th block as follows for $j \in [N]$,

$$[\Phi((X, X'), (\mathcal{X}, \mathcal{X}'))]_{1,j} = \phi((X, X'), (X_j, X'_j)).$$

Remarks. The kernel Φ is in fact what $\hat{\Phi}_0$ converges to as the neural net width approaches infinity. However, $\hat{\Phi}_0 \equiv \hat{\Phi}_0((\mathcal{X}, \mathcal{X}'), (\mathcal{X}, \mathcal{X}'))$ depends on \mathcal{Y} and \mathcal{Y}' , while $\Phi \equiv \Phi((\mathcal{X}, \mathcal{X}'), (\mathcal{X}, \mathcal{X}'))$ does not, since the terms in Φ that depend on \mathcal{Y} or \mathcal{Y}' all vanish as the width approaches infinity. Besides, (11) is a sum of two kernel regression terms, but it can be viewed as a single special kernel regression. Notably, the MNK function Φ can be seen as a *composite* kernel function built on the base kernel function Θ .

6 Experimental Results on Few-Shot Classification

The MNK-based kernel regression demonstrated in Theorem 3 can be viewed as a kernel-based meta-learning method. To study it empirically, we apply it to a popular few-shot classification benchmark, the Omniglot dataset [24], and compare it against MAML [11], a standard GBML method, and implicit MAML (iMAML) [38], a recently proposed variant of MAML with better performance. Although these methods are not state-of-the-art on the Omniglot benchmark, they provide an apples-to-apples comparison for MNK, which is an induced kernel of MAML in the infinite width limit.

Details of Dataset and Classification Setup. The Omniglot dataset contains 1623 handwritten characters from 50 alphabets. For each character, the dataset provides 20 image instances, in which each instance is handwritten by a unique person. A normal protocol of few-shot learning is to select 1200 characters for training and the remaining 423 characters for test [11], then to perform k -way n -shot classification. The setup of k -way n -shot classification is: randomly take k classes (i.e., characters in Omniglot), then provide n different samples with labels of each class to the few-shot learning model (e.g., GBML model), and finally evaluate the model's performance on classifying the rest samples (i.e., $(20 - n)$ samples in the case of Omniglot) in these k classes. Note the n and k used here is consistent with our definition of them in Sec 2.1.

Data Preprocessing. Since we derive the MNK-based kernel method in the regression setting with ℓ_2 loss, we have to perform label preprocessing in order to apply this kernel method to few-shot multi-class classification. The reason for that is demonstrated below. The application of kernel regression on multi-class classification [36] usually uses one-hot encoding, a one-to-one mapping on digital labels. However, it fails in the case of kernel regression on *few-shot* multi-class classification, since each classification task (e.g., training or test task) has its own classes of labels. For instance, in 5-way n -shot classification, a task assigns digital labels $\{1, 2, 3, 4, 5\}$ to its samples, but another task also has 5 classes of samples, so it assigns the same digital labels, $\{1, 2, 3, 4, 5\}$, to its samples. Then, different classes from multiple tasks share the same digital labels, which is ill-defined in the setting of kernel regression⁴. To resolve this issue, we design a label preprocessing technique that projects digital labels from different tasks into a single vector space. Specifically, we first choose a fixed feature extractor ψ such that it can transform any sample x into a feature vector, $\psi(x) \in \mathbb{R}^h$, in a h -d Euclidean space. Then, we use this feature extractor to convert all samples in each training task into feature vectors. For test tasks, we do this for support samples only. After that, in each task,

⁴We will provide specific examples in Appendix F to explain why one-hot or digital labels are ill-defined for kernel regression on few-shot classification.

# Characters	5	10	20	40	80
% of Omniglot	0.42%	0.83%	1.67%	3.33%	6.67%
MAML	78.7 \pm 2.1	83.2 \pm 1.3	85.9 \pm 1.1	88.3 \pm 0.7	90.9 \pm 0.6
iMAML	73.4 \pm 2.4	79.0 \pm 2.2	85.0 \pm 1.4	89.5 \pm 0.5	92.6 \pm 0.6
MNK	82.6 \pm 0.6	84.9 \pm 0.8	88.0 \pm 0.7	90.1 \pm 0.4	91.7 \pm 0.5

Table 1: Test accuracy for 5-way 1-shot classification on Omniglot. The “# Characters” means the number of characters in the training set of each experiment. In normal protocols on Omniglot, the number of characters for meta-training is 1200, hence “% of Omniglot” = $\frac{\text{\# Characters}}{1200}$, representing the size of each subset of Omniglot. The lower three rows records test accuracy in percentage for MAML, iMAML and MNK, separately, with digits after \pm as the standard deviation over 10 random seeds. Bold digits represent the highest accuracy among these methods.

we compute the centroids of feature vectors corresponding to samples in each class (i.e., obtain five centroids for the five classes in each task), and use the centroid (i.e., a h -d vector) of each class as its new label. In this way, classes from various tasks are marked by different vector labels, which are well-defined for kernel regression. For convenience, we train a randomly initialized CNN over all training data in the *supervised learning* way, and take its hidden layers as the feature extractor. Details about this feature extractor can be found in Appendix F.

Computation of Meta Neural Kernels. Theorem 3 shows that to compute the MNK, Φ , we need access to the base kernel function, Θ . We choose CNTK⁵ from [3] as Θ , since it is a kernel function derived from convolutional neural networks, the default neural networks for GBML on Omniglot. Note that the calculation of Φ requires computation and memory cost of $\mathcal{O}(n^2 N^2)$ because $\Phi \in \mathbb{R}^{knN \times knN}$. This quadratic cost makes it computation expensive to apply the MNK-based kernel-method to few-shot classifications with a large number of training data (i.e., large N or n). For instance, computing the MNK on the full Omniglot dataset will take about 3000 GPU hours on NVIDIA RTX 2080ti.

Implementation Details. We implement our MNK method in Python, in combination with the CUDA code from [3]. For the MAML code, we adopt a popular PyTorch implementation⁶ from [15]. For a fair comparison, we adopt a PyTorch implementation⁷ of iMAML based on [15].

Small-Data Few-Shot Classification. Due to our limited computation resource, we can only conduct experiments on subsets of the Omniglot dataset. Specifically, we randomly take 200 characters as the fixed dataset for meta-test, where each character contains 20 image samples. Then, we randomly select subsets with varying sizes from the remaining Omniglot characters for meta-training. We consider the standard 5-way 1-shot classification setting to compare the performance of MNK vs. MAML & iMAML. For each experiment, we run it over 10 random seeds, and each seed determines a unique randomly selected meta-training dataset. The test performance of MNK, MAML and iMAML is summarized in Table 1.

Performance Comparison. From Table 1, we can observe that our MNK method outperforms MAML and iMAML in the case of *small training data*. Specifically, when # Characters = 5, 10, 20, 40, the MNK method achieves higher test accuracy than MAML and iMAML. As the size of the meta-training set keeps increasing (i.e., # Characters \geq 80), MNK is outperformed by GBML methods. These results suggest that our MNK method is suitable for the case of *small training data*, which is actually a realistic scenario of many real-world problems. In addition, we provide an ablation study on the effect of the label preprocessing operation on MAML in Appendix F, and we find the label preprocessing cannot improve MAML performance, indicating the decent performance of MNK is not because of the additional information provided by the preprocessed labels.

Extendability and Scalability. Sec. 5 shows that MNK is a meta-level composite kernel built upon a base kernel function. In this paper, we adopt CNTK as the base kernel function [3]. However, one can replace CNTK with other kernel functions. It is possible that using base kernels with better performance on image classification (e.g., [28, 39]) can increase the MNK performance on few-shot image classification. On the other hand, in large-data cases, one can apply approximation techniques

⁵We adopt the CUDA implementation released by [3] at <https://github.com/ruosongwang/CNTK>.

⁶<https://github.com/facebookresearch/higher/blob/master/examples/maml-omniglot.py>

⁷<https://github.com/prolearner/hypertorch>

for large kernels such as random features [37, 32], which reduce the quadratic computation to a linear one, at the cost of decreased test accuracy.

More Details. We provide more details about the experiments in Appendix F, including an ablation study on the label preprocessing operation.

7 Conclusion

In this paper, we theoretically study the properties of gradient-based meta-learning (GBML), a popular family of meta-learning methods usually applied with deep neural networks (DNNs). We provide theoretical guarantees on the global convergence of GBML with over-parameterized DNNs. We also demonstrate an equivalence between GBML and a functional gradient descent operation, which provides a theoretical verification of the intuition behind the design of GBML. Finally, we show with extreme over-parameterization, GBML is equivalent to a kernel regression, which outperforms standard GBML with DNNs on few-shot image classification tasks, in the *small data* case.

Acknowledgements

H. Wang would like to thank Simon Du, Niao He, Han Liu, Yunan Luo and Ruosong Wang for insightful discussions.

References

- [1] Z. Allen-Zhu, Y. Li, and Z. Song. A convergence theory for deep learning via over-parameterization. *International Conference on Machine Learning*, 2019.
- [2] S. Arora, S. Du, W. Hu, Z. Li, and R. Wang. Fine-grained analysis of optimization and generalization for overparameterized two-layer neural networks. In *International Conference on Machine Learning*, pages 322–332, 2019.
- [3] S. Arora, S. S. Du, W. Hu, Z. Li, R. Salakhutdinov, and R. Wang. On exact computation with an infinitely wide neural net. *NeurIPS*, 2019.
- [4] S. Arora, S. S. Du, Z. Li, R. Salakhutdinov, R. Wang, and D. Yu. Harnessing the power of infinitely wide deep nets on small-data tasks. In *International Conference on Learning Representations*, 2020.
- [5] M.-F. Balcan, M. Khodak, and A. Talwalkar. Provable guarantees for gradient-based meta-learning. In *International Conference on Machine Learning*, pages 424–433, 2019.
- [6] Y. Burda, H. Edwards, A. Storkey, and O. Klimov. Exploration by random network distillation. In *International Conference on Learning Representations*, 2019.
- [7] J. Deng, W. Dong, R. Socher, L.-J. Li, K. Li, and L. Fei-Fei. ImageNet: A Large-Scale Hierarchical Image Database. In *CVPR*, 2009.
- [8] S. S. Du, J. D. Lee, H. Li, L. Wang, and X. Zhai. Gradient descent finds global minima of deep neural networks. *International Conference on Machine Learning*, 2019.
- [9] A. Fallah, A. Mokhtari, and A. Ozdaglar. On the convergence theory of gradient-based model-agnostic meta-learning algorithms. In *International Conference on Artificial Intelligence and Statistics*, pages 1082–1092, 2020.
- [10] C. Finn. *Learning to Learn with Gradients*. PhD thesis, EECS Department, University of California, Berkeley, Aug 2018.
- [11] C. Finn, P. Abbeel, and S. Levine. Model-agnostic meta-learning for fast adaptation of deep networks. In *Proceedings of the 34th International Conference on Machine Learning-Volume 70*, pages 1126–1135. JMLR. org, 2017.
- [12] C. Finn, A. Rajeswaran, S. Kakade, and S. Levine. Online meta-learning. In *International Conference on Machine Learning*, pages 1920–1930, 2019.
- [13] C. Finn, K. Xu, and S. Levine. Probabilistic model-agnostic meta-learning. In *Advances in Neural Information Processing Systems*, pages 9516–9527, 2018.

- [14] S. Flennerhag, A. A. Rusu, R. Pascanu, F. Visin, H. Yin, and R. Hadsell. Meta-learning with warped gradient descent. In *International Conference on Learning Representations*, 2020.
- [15] E. Grefenstette, B. Amos, D. Yarats, P. M. Htut, A. Molchanov, F. Meier, D. Kiela, K. Cho, and S. Chintala. Generalized inner loop meta-learning. *arXiv preprint arXiv:1910.01727*, 2019.
- [16] Y. Hu, S. Zhang, X. Chen, and N. He. Biased stochastic gradient descent for conditional stochastic optimization. *arXiv preprint arXiv:2002.10790*, 2020.
- [17] A. Jacot, F. Gabriel, and C. Hongler. Neural tangent kernel: Convergence and generalization in neural networks. In *Advances in neural information processing systems*, pages 8571–8580, 2018.
- [18] A. Jacot, F. Gabriel, and C. Hongler. The asymptotic spectrum of the hessian of dnn throughout training. In *International Conference on Learning Representations*, 2020.
- [19] K. Ji, J. Yang, and Y. Liang. Multi-step model-agnostic meta-learning: Convergence and improved algorithms. *arXiv preprint arXiv:2002.07836*, 2020.
- [20] Z. Ji and M. Telgarsky. Gradient descent aligns the layers of deep linear networks. In *International Conference on Learning Representations*, 2019.
- [21] B. Kågström. Bounds and perturbation bounds for the matrix exponential. *BIT Numerical Mathematics*, 17(1):39–57, 1977.
- [22] K. Kawaguchi and L. P. Kaelbling. Elimination of all bad local minima in deep learning. *arXiv preprint arXiv:1901.00279*, 2019.
- [23] M. Khodak, M.-F. F. Balcan, and A. S. Talwalkar. Adaptive gradient-based meta-learning methods. In *Advances in Neural Information Processing Systems*, pages 5915–5926, 2019.
- [24] B. M. Lake, R. Salakhutdinov, and J. B. Tenenbaum. Human-level concept learning through probabilistic program induction. *Science*, 350(6266):1332–1338, 2015.
- [25] J. Lee, L. Xiao, S. S. Schoenholz, Y. Bahri, J. Sohl-Dickstein, and J. Pennington. Wide neural networks of any depth evolve as linear models under gradient descent. *NeurIPS*, 2019.
- [26] D. Li, T. Ding, and R. Sun. On the benefit of width for neural networks: Disappearance of bad basins. *arXiv preprint arXiv:1812.11039*, 2018.
- [27] Y. Li and Y. Liang. Learning overparameterized neural networks via stochastic gradient descent on structured data. In *Advances in Neural Information Processing Systems*, pages 8157–8166, 2018.
- [28] Z. Li, R. Wang, D. Yu, S. S. Du, W. Hu, R. Salakhutdinov, and S. Arora. Enhanced convolutional neural tangent kernels. *arXiv preprint arXiv:1911.00809*, 2019.
- [29] S. Liang, R. Sun, J. D. Lee, and R. Srikant. Adding one neuron can eliminate all bad local minima. In *Advances in Neural Information Processing Systems*, pages 4355–4365, 2018.
- [30] S. Liang, R. Sun, Y. Li, and R. Srikant. Understanding the loss surface of neural networks for binary classification. In *International Conference on Machine Learning*, pages 2835–2843, 2018.
- [31] S. Liang, R. Sun, and R. Srikant. Revisiting landscape analysis in deep neural networks: Eliminating decreasing paths to infinity. *arXiv preprint arXiv:1912.13472*, 2019.
- [32] F. Liu, X. Huang, Y. Chen, and J. A. Suykens. Random features for kernel approximation: A survey in algorithms, theory, and beyond. *arXiv preprint arXiv:2004.11154*, 2020.
- [33] Q. Nguyen, M. C. Mukkamala, and M. Hein. On the loss landscape of a class of deep neural networks with no bad local valleys. In *International Conference on Learning Representations*, 2019.
- [34] A. Nichol, J. Achiam, and J. Schulman. On first-order meta-learning algorithms. *arXiv preprint arXiv:1803.02999*, 2018.
- [35] E. Park and J. B. Oliva. Meta-curvature. In *Advances in Neural Information Processing Systems*, pages 3309–3319. Curran Associates, Inc., 2019.
- [36] F. Pedregosa, G. Varoquaux, A. Gramfort, V. Michel, B. Thirion, O. Grisel, M. Blondel, P. Prettenhofer, R. Weiss, V. Dubourg, J. Vanderplas, A. Passos, D. Cournapeau, M. Brucher, M. Perrot, and E. Duchesnay. Scikit-learn: Machine learning in Python. *Journal of Machine Learning Research*, 12:2825–2830, 2011.

- [37] A. Rahimi and B. Recht. Random features for large-scale kernel machines. In *Advances in neural information processing systems*, pages 1177–1184, 2008.
- [38] A. Rajeswaran, C. Finn, S. M. Kakade, and S. Levine. Meta-learning with implicit gradients. In *Advances in Neural Information Processing Systems*, pages 113–124, 2019.
- [39] V. Shankar, A. Fang, W. Guo, S. Fridovich-Keil, L. Schmidt, J. Ragan-Kelley, and B. Recht. Neural kernels without tangents. *ICML*, 2020.
- [40] R. Sun. Optimization for deep learning: theory and algorithms. *arXiv preprint arXiv:1912.08957*, 2019.
- [41] J. Vanschoren. Meta-learning: A survey. *arXiv preprint arXiv:1810.03548*, 2018.
- [42] O. Vinyals, C. Blundell, T. Lillicrap, D. Wierstra, et al. Matching networks for one shot learning. In *Advances in neural information processing systems*, pages 3630–3638, 2016.
- [43] L. Wang, Q. Cai, Z. Yang, and Z. Wang. On the global optimality of model-agnostic meta-learning. In *International Conference on Machine Learning*, pages 101–110, 2020.
- [44] R. Xu, L. Chen, and A. Karbasi. Meta learning in the continuous time limit. *arXiv preprint arXiv:2006.10921*, 2020.
- [45] P. Zhou, X. Yuan, H. Xu, and S. Yan. Efficient meta learning via minibatch proximal update. *Neural Information Processing Systems*, 2019.

A Neural Network Setup and Supervised Learning

In this paper, we consider a fully-connected feed-forward network with L hidden layers. Each hidden layer has width l_i , for $i = 1, \dots, L$. The readout layer (i.e. output layer) has width $l_{L+1} = k$. At each layer i , for arbitrary input $x \in \mathbb{R}^d$, we denote the pre-activation and post-activation functions by $h^i(x), z^i(x) \in \mathbb{R}^{l_i}$. The relations between layers in this network are

$$\begin{cases} h^{i+1} &= z^i W^{i+1} + b^{i+1} \\ z^{i+1} &= \sigma(h^{i+1}) \end{cases} \quad \text{and} \quad \begin{cases} W_{\mu,\nu}^i &= \omega_{\mu\nu}^i \sim \mathcal{N}(0, \frac{\sigma_\omega}{\sqrt{l_i}}) \\ b_\nu^i &= \beta_\nu^i \sim \mathcal{N}(0, \sigma_b) \end{cases}, \quad (15)$$

where $W^{i+1} \in \mathbb{R}^{l_i \times l_{i+1}}$ and $b^{i+1} \in \mathbb{R}^{l_{i+1}}$ are the weight and bias of the layer, $\omega_{\mu\nu}^i$ and b_ν^i are trainable variables drawn i.i.d. from zero-mean Gaussian distributions at initialization (i.e., $\frac{\sigma_\omega}{\sqrt{l_i}}$ and σ_b^2 are variances for weight and bias, and σ is a point-wise activation function).

A.1 Global Convergence of Supervised Learning with Deep Neural Networks

Recently, there is a line of works studying the optimization of neural networks in the setting of supervised learning (e.g. [1, 8, 17, 3, 25, 20, 2, 21, 21, 21, 27, 31, 29, 30, 22, 26, 33]), and it has been proved that the optimization is guaranteed to converge to global optima; see [40] for an overview. Below, we briefly discuss one such convergence result.

Consider a supervised learning task: given the training samples $X = (x_i)_{i=1}^n$ and targets $Y = (y_i)_{i=1}^n$, we learn the neural network f by minimizing

$$L(\theta) = \sum_{i=1}^n \ell(f_\theta(x_i), y_i) = \frac{1}{2} \|f_\theta(X) - Y\|_2^2, \quad (16)$$

where $\ell(\hat{y}, y) = \frac{1}{2} \|\hat{y} - y\|_2^2$ is the loss function, and $f_\theta(X) \equiv (f_\theta(x_i))_{i=1}^n \in \mathbb{R}^{kn}$ is the concatenated network outputs on all samples.

The update rule of gradient descent on L is standard:

$$\theta_{t+1} = \theta_t - \lambda \nabla_{\theta_t} L(\theta_t)$$

where t represents the number of training steps.

With sufficiently small learning rate λ and sufficiently large network width, [17, 25, 3] show that the gradient descent is guaranteed to obtain zero training loss given long enough training time, i.e., $\lim_{t \rightarrow \infty} L(\theta_t) = 0$. Currently, the global convergence of supervised learning with deep neural networks is mostly restricted to ℓ_2 loss. Other loss functions are generally harder to analyze. For example, with cross-entropy loss function, the model parameters do not converge to a point without regularization. This is the reason why we also consider ℓ_2 loss.

B Proof of Global Convergence for Gradient-Based Meta-Learning with Deep Neural Networks

In this section, we will prove Theorem 2, which states that with sufficiently over-parameterized neural networks, gradient-based meta-learning trained under gradient descent is guaranteed to converge to global optima at linear convergence rate.

We consider the standard parameterization scheme of neural networks shown in (15).

Theorem 2 depends on several assumptions and lemmas. The assumptions are listed below. After that, we present the lemmas and the global convergence theorem, with proofs in Appendix B.1, B.2, B.3 and B.4. For Corollary 2.1, we append its proof to Appendix C.

Assumption 1 (Bounded Input Norm). $\forall X \in \mathcal{X}$, for any sample $x \in X$, $\|x\|_2 \leq 1$. Similarly, $\forall X' \in \mathcal{X}'$, for any sample $x' \in X'$, $\|x'\| \leq 1$. (This is equivalent to a input normalization operation, which is common in data preprocessing.)

Assumption 2 (Non-Degeneracy). The meta-training set $(\mathcal{X}, \mathcal{Y})$ and the meta-test set $(\mathcal{X}', \mathcal{Y}')$ are both contained in some compact set. Also, \mathcal{X} and \mathcal{X}' are both non-degenerate, i.e. $\forall X, \tilde{X} \in \mathcal{X}$, $X \neq \tilde{X}$, and $\forall X', \tilde{X}' \in \mathcal{X}'$, $X' \neq \tilde{X}'$.

Assumption 3 (Same Width for Hidden Layers). *All hidden layers share the same width, l , i.e., $l_1 = l_2 = \dots = l_L = l$.*

Assumption 4 (Activation Function). *The activation function used in neural networks, ϕ , has the following properties:*

$$|\phi(0)| < \infty, \quad \|\phi'\|_\infty < \infty, \quad \sup_{x \neq \tilde{x}} |\phi'(x) - \phi'(\tilde{x})|/|x - \tilde{x}| < \infty. \quad (17)$$

Assumption 5 (Full-Rank). *The kernel Φ defined in Lemma 6 is full-rank.*

These assumptions are common, and one can find similar counterparts of them in the literature for supervised learning [25, 3].

As defined in the main text, θ is used to represent the neural net parameters. For convenience, we define some short-hand notations:

$$f_t(\cdot) = f_{\theta_t}(\cdot) \quad (18)$$

$$F_t(\cdot) = F_{\theta_t}(\cdot) \quad (19)$$

$$f(\theta) = f_\theta(\mathcal{X}) = ((f_\theta(X_i))_{i=1}^N \quad (20)$$

$$F(\theta) = F_\theta(\mathcal{X}, \mathcal{X}', \mathcal{Y}') = ((F_\theta(X_i, X'_i, Y'_i))_{i=1}^N \quad (21)$$

$$g(\theta) = F_\theta(\mathcal{X}, \mathcal{X}', \mathcal{Y}') - \mathcal{Y} \quad (22)$$

$$J(\theta) = \nabla_\theta F(\theta) = \nabla_\theta F_\theta(\mathcal{X}, \mathcal{X}', \mathcal{Y}') \quad (23)$$

and

$$\mathcal{L}(\theta_t) = \ell(F(\theta_t), \mathcal{Y}) = \frac{1}{2} \|g(\theta_t)\|_2^2 \quad (24)$$

$$\hat{\Phi}_t = \frac{1}{l} \nabla F_{\theta_t}(\mathcal{X}, \mathcal{X}', \mathcal{Y}') \nabla F_{\theta_t}(\mathcal{X}, \mathcal{X}', \mathcal{Y}')^\top = \frac{1}{l} J(\theta) J(\theta)^\top \quad (25)$$

where we use the ℓ_2 loss function $\ell(\hat{y}, y) = \frac{1}{2} \|\hat{y} - y\|_2^2$ in the definition of training loss $\mathcal{L}(\theta_t)$ in (24), and the $\hat{\Phi}_t$ in (25) is based on the definition⁸ of $\hat{\Phi}_\theta(\cdot, \star)$ in Sec. 3.

Below, Lemma 1 proves the Jacobian J is locally Lipschitz, Lemma 5 proves the training loss at initialization is bounded, and Lemma 6 proves $\hat{\Phi}_0$ converges in probability to a deterministic kernel matrix with bounded positive eigenvalues. Finally, with these lemmas, we can prove the global convergence of GBML in Theorem 7.

Lemma 4 (Local Lipschitzness of Jacobian) (Lemma 1 restated). *Suppose⁹ $\tau = \mathcal{O}(\frac{1}{\lambda})$, then there exists $K > 0$ such that: $\forall C > 0$, the following inequalities hold true with high probability over random initialization,*

$$\forall \theta, \bar{\theta} \in B(\theta_0, Cl^{-\frac{1}{2}}), \begin{cases} \frac{1}{\sqrt{l}} \|J(\theta) - J(\bar{\theta})\|_F & \leq K \|\theta - \bar{\theta}\|_2 \\ \frac{1}{\sqrt{l}} \|J(\theta)\|_F & \leq K \end{cases} \quad (26)$$

where B is a neighborhood defined as

$$B(\theta_0, R) := \{\theta : \|\theta - \theta_0\|_2 < R\}. \quad (27)$$

Proof. See Appendix B.1. □

Lemma 5 (Bounded Initial Loss). *For arbitrarily small $\delta_0 > 0$, there are constants $R_0 > 0$ and $l^* > 0$ such that as long as the width $l > l^*$, with probability at least $(1 - \delta_0)$ over random initialization,*

$$\|g(\theta_0)\|_2 = \|F_{\theta_0}(\mathcal{X}, \mathcal{X}', \mathcal{Y}') - \mathcal{Y}\|_2 \leq R_0, \quad (28)$$

⁸There is a typo in the definition of $\hat{\Phi}_\theta(\cdot, \star)$ in Sec. 3: a missing factor $\frac{1}{l}$. The correct definition should be $\hat{\Phi}_\theta(\cdot, \star) = \frac{1}{l} \nabla_\theta F_\theta(\cdot) \nabla_\theta F_\theta(\star)^\top$. Similarly, the definition of Φ in Theorem 2 also missis this factor: the correct version is $\Phi = \frac{1}{l} \lim_{l \rightarrow \infty} J(\theta_0) J(\theta_0)^\top$

⁹This assumption is realistic in practice. For example, the official implementation of MAML [11] for few-shot classification benchmarks adopts (i) $\tau = 1, \lambda = 0.4$ and (ii) $\tau = 5, \lambda = 0.1$, which both satisfy our assumption.

which is also equivalent to

$$\mathcal{L}(\theta_0) = \frac{1}{2} \|g(\theta_0)\|_2^2 \leq \frac{1}{2} R_0^2.$$

Proof. See Appendix B.2. \square

Lemma 6 (Kernel Convergence). *Suppose the learning rates η and λ sufficiently small. As the network width l approaches infinity, $\hat{\Phi}_0 = J(\theta_0)J(\theta_0)^\top$ converges in probability to a deterministic kernel matrix Φ (i.e., $\Phi = \lim_{l \rightarrow \infty} \hat{\Phi}_0$), which is independent of θ_0 and can be analytically calculated. Furthermore, the eigenvalues of Φ is bounded as, $0 < \sigma_{\min}(\Phi) \leq \sigma_{\max}(\Phi) < \infty$.*

Proof. See Appendix B.3. \square

Note the update rule of gradient descent on θ_t with learning rate η can be expressed as

$$\theta_{t+1} = \theta_t - \eta J(\theta_t)^\top g(\theta_t). \quad (29)$$

The following theorem proves the global convergence of GBML under the update rule of gradient descent.

Theorem 7 (Global Convergence (Theorem 2 restated)). *Suppose $\tau = \mathcal{O}(\frac{1}{\lambda})$. Denote $\sigma_{\min} = \sigma_{\min}(\Phi)$ and $\sigma_{\max} = \sigma_{\max}(\Phi)$. For any $\delta_0 > 0$ and $\eta_0 < \frac{2}{\sigma_{\max} + \sigma_{\min}}$, there exist $R_0 > 0$, $\Lambda \in \mathbb{N}$, $K > 1$, and $\lambda_0 > 0$, such that: for width $l \geq \Lambda$, running gradient descent with learning rates $\eta = \frac{\eta_0}{l}$ and $\lambda < \frac{\lambda_0}{l}$ over random initialization, the following inequalities hold true with probability at least $(1 - \delta_0)$:*

$$\sum_{j=1}^t \|\theta_j - \theta_{j-1}\|_2 \leq \frac{3KR_0}{\sigma_{\min}} l^{-\frac{1}{2}} \quad (30)$$

$$\sup_t \|\hat{\Phi}_0 - \hat{\Phi}_t\|_F \leq \frac{6K^3 R_0}{\sigma_{\min}} l^{-\frac{1}{2}} \quad (31)$$

and

$$g(\theta_t) = \|F(\theta_t) - \mathcal{Y}\|_2 \leq \left(1 - \frac{\eta_0 \sigma_{\min}}{3}\right)^t R_0, \quad (32)$$

which leads to

$$\mathcal{L}(\theta_t) = \frac{1}{2} \|F(\theta_t) - \mathcal{Y}\|_2^2 \leq \left(1 - \frac{\eta_0 \sigma_{\min}}{3}\right)^{2t} \frac{R_0^2}{2}, \quad (33)$$

indicating the training loss converges to zero at a linear rate.

Proof. See Appendix B.4. \square

In the results of Theorem 7 above, (30) considers the optimization trajectory of network parameters, and show the parameters move locally during training. (31) indicates the kernel matrix $\hat{\Phi}_t$ changes slowly. Finally, (33) demonstrates that the training loss of GBML decays exponentially to zero as the training time evolves, indicating convergence to global optima at a linear rate.

B.1 Proof of Lemma 4

Proof of Lemma 4. Consider an arbitrary task $\mathcal{T} = (X, Y, X', Y')$. Given sufficiently large width l , for any parameters in the neighborhood of the initialization, i.e., $\theta \in B(\theta_0, Cl^{-1/2})$, based on [25], we know the meta-output can be decomposed into a terms of f_θ ,

$$F_\theta(X, X', Y') = f_\theta(X) - \hat{\Theta}_\theta(X, X') \hat{\Theta}_\theta^{-1} (I - e^{-\lambda \hat{\Theta}_\theta \tau}) (f_\theta(X') - Y'), \quad (34)$$

where $\hat{\Theta}_\theta(X, X') = \frac{1}{l} \nabla_\theta f_\theta(X) \nabla_\theta f_\theta(X')^\top$, and $\hat{\Theta}_\theta \equiv \hat{\Theta}_\theta(X', X')$ for convenience.

Then, we consider $\nabla_{\theta} F_{\theta}(X, X', Y')$, the gradient of $F_{\theta}(X, X', Y')$ in (34). Since [18] shows that the Hessian of any sufficiently wide neural network has almost zero operator norm, i.e. $\|\nabla_{\theta}^2 f_{\theta}(\cdot)\|_{\text{op}} \simeq 0$, we can drop the Hessian terms appearing in $\nabla_{\theta} F_{\theta}(X, X', Y')$, resulting in

$$\nabla_{\theta} F_{\theta}(X, X', Y') = \nabla_{\theta} f_{\theta}(X) - \hat{\Theta}_{\theta}(X, X') \hat{\Theta}_{\theta}^{-1} (I - e^{-\lambda \hat{\Theta}_{\theta} \tau}) \nabla_{\theta} f_{\theta}(X'). \quad (35)$$

Now, let us consider the SVD decomposition on $\frac{1}{\sqrt{l}} \nabla_{\theta} f_{\theta}(X') \in \mathbb{R}^{km \times D}$, where $X' \in \mathbb{R}^{k \times m}$ and $\theta \in \mathbb{R}^D$. such that $\frac{1}{\sqrt{l}} \nabla_{\theta} f_{\theta}(X') = U \Sigma V^{\top}$, where $U \in \mathbb{R}^{km \times km}$, $V \in \mathbb{R}^{D \times km}$ are orthonormal matrices while $\Sigma \in \mathbb{R}^{km \times km}$ is a diagonal matrix. Note that we take $km \leq D$ here since the width is sufficiently wide.

Then, since $\hat{\Theta}_{\theta} = \frac{1}{l} \nabla_{\theta} f_{\theta}(X') \nabla_{\theta} f_{\theta}(X')^{\top} = U \Sigma V^{\top} V \Sigma U^{\top} = U \Sigma^2 U^{\top}$, we have $\hat{\Theta}_{\theta}^{-1} = U \Sigma^{-2} U^{\top}$. Also, by Taylor expansion, we have

$$I - e^{-\lambda \hat{\Theta}_{\theta} \tau} = I - \sum_{i=0}^{\infty} \frac{(-\lambda \tau)^i}{i!} (\hat{\Theta}_{\theta})^i = U \left(I - \sum_{i=0}^{\infty} \frac{(-\lambda \tau)^i}{i!} (\Sigma)^i \right) U^{\top} = U (I - e^{-\lambda \Sigma \tau}) U^{\top}. \quad (36)$$

With these results of SVD, (35) becomes

$$\begin{aligned} \nabla_{\theta} F((X, X', Y'), \theta) &= \nabla_{\theta} f_{\theta}(X) - \frac{1}{l} \nabla_{\theta} f_{\theta}(X) \nabla_{\theta} f_{\theta}(X')^{\top} \hat{\Theta}_{\theta}^{-1} (I - e^{-\lambda \hat{\Theta}_{\theta} \tau}) \nabla_{\theta} f_{\theta}(X') \\ &= \nabla_{\theta} f_{\theta}(X) - \frac{1}{l} \nabla_{\theta} f_{\theta}(X) (\sqrt{l} V \Sigma U^{\top}) (U \Sigma^{-2} U^{\top}) [U (I - e^{-\lambda \Sigma \tau}) U^{\top}] (\sqrt{l} U \Sigma V^{\top}) \\ &= \nabla_{\theta} f_{\theta}(X) - \nabla_{\theta} f_{\theta}(X) V \Sigma^{-1} (I - e^{-\lambda \Sigma \tau}) \Sigma V^{\top} \\ &= \nabla_{\theta} f_{\theta}(X) - \nabla_{\theta} f_{\theta}(X) V (I - e^{-\lambda \Sigma \tau}) V^{\top} \\ &= \nabla_{\theta} f_{\theta}(X) - \nabla_{\theta} f_{\theta}(X) (I - e^{-\lambda H_{\theta} \tau}) \\ &= \nabla_{\theta} f_{\theta}(X) e^{-\lambda H_{\theta} \tau} \end{aligned} \quad (37)$$

where $H_{\theta} \equiv H_{\theta}(X', X') = \frac{1}{l} \nabla_{\theta} f_{\theta}(X')^{\top} \nabla_{\theta} f_{\theta}(X') \in \mathbb{R}^{D \times D}$, and the step (37) can be easily obtained by a Taylor expansion similar to (36).

Note that H_{θ} is a product of $\nabla_{\theta} f_{\theta}(X')^{\top}$ and its transpose, hence it is positive semi-definite, and so does $e^{-\lambda H_{\theta} \tau}$. By eigen-decomposition on H , we can easily see that the eigenvalues of $e^{-\lambda H_{\theta} \tau}$ are all in the range $[0, 1)$ for arbitrary $\tau > 0$. Therefore, it is easy to get that for arbitrary $\tau > 0$,

$$\|\nabla_{\theta} F((X, X', Y'), \theta)\|_F = \|\nabla_{\theta} f_{\theta}(X) e^{-\lambda H_{\theta} \tau}\|_F \leq \|\nabla_{\theta} f_{\theta}(X)\|_F \quad (38)$$

By Lemma 1 of [25], we know that there exists a $K_0 > 0$ such that for any X and θ ,

$$\left\| \frac{1}{\sqrt{l}} \nabla f_{\theta}(X) \right\|_F \leq K_0. \quad (39)$$

Combining (38) and (39), we have

$$\left\| \frac{1}{\sqrt{l}} \nabla_{\theta} F((X, X', Y'), \theta) \right\|_F \leq \left\| \frac{1}{\sqrt{l}} \nabla_{\theta} f_{\theta}(X) \right\|_F \leq K_0, \quad (40)$$

which is equivalent to

$$\frac{1}{\sqrt{l}} \|J(\theta)\|_F \leq K_0 \quad (41)$$

Now, let us study the other term of interest, $\|J(\theta) - J(\bar{\theta})\|_F = \left\| \frac{1}{\sqrt{l}} \nabla_{\theta} F((X, X', Y'), \theta) - \frac{1}{\sqrt{l}} \nabla_{\theta} F((X, X', Y'), \bar{\theta}) \right\|_F$, where $\theta, \bar{\theta} \in B(\theta_0, Cl^{-1/2})$.

To bound $\|J(\theta) - J(\bar{\theta})\|_F$, let us consider

$$\|\nabla_{\theta} F((X, X', Y'), \theta) - \nabla_{\bar{\theta}} F((X, X', Y'), \bar{\theta})\|_{op} \quad (42)$$

$$\begin{aligned} &= \|\nabla_{\theta} f_{\theta}(X) e^{-\lambda H_{\theta} \tau} - \nabla_{\bar{\theta}} f_{\bar{\theta}}(X) e^{-\lambda H_{\bar{\theta}} \tau}\|_{op} \\ &= \frac{1}{2} \|(\nabla_{\theta} f_{\theta}(X) - \nabla_{\bar{\theta}} f_{\bar{\theta}}(X)) (e^{-\lambda H_{\theta} \tau} + e^{-\lambda H_{\bar{\theta}} \tau}) \\ &\quad + (\nabla_{\theta} f_{\theta}(X) + \nabla_{\bar{\theta}} f_{\bar{\theta}}(X)) (e^{-\lambda H_{\theta} \tau} - e^{-\lambda H_{\bar{\theta}} \tau})\|_{op} \end{aligned} \quad (43)$$

$$\leq \frac{1}{2} \|\nabla_{\theta} f_{\theta}(X) - \nabla_{\bar{\theta}} f_{\bar{\theta}}(X)\|_{op} \|e^{-\lambda H_{\theta} \tau} + e^{-\lambda H_{\bar{\theta}} \tau}\|_{op} \quad (44)$$

$$\begin{aligned} &+ \frac{1}{2} \|\nabla_{\theta} f_{\theta}(X) + \nabla_{\bar{\theta}} f_{\bar{\theta}}(X)\|_{op} \|e^{-\lambda H_{\theta} \tau} - e^{-\lambda H_{\bar{\theta}} \tau}\|_{op} \\ &\leq \frac{1}{2} \|\nabla_{\theta} f_{\theta}(X) - \nabla_{\bar{\theta}} f_{\bar{\theta}}(X)\|_{op} (\|e^{-\lambda H_{\theta} \tau}\|_{op} + \|e^{-\lambda H_{\bar{\theta}} \tau}\|_{op}) \end{aligned} \quad (45)$$

$$+ \frac{1}{2} (\|\nabla_{\theta} f_{\theta}(X)\|_{op} + \|\nabla_{\bar{\theta}} f_{\bar{\theta}}(X)\|_{op}) \|e^{-\lambda H_{\theta} \tau} - e^{-\lambda H_{\bar{\theta}} \tau}\|_{op} \quad (46)$$

It is obvious that $\|e^{-\lambda H_{\theta} \tau}\|_{op}, \|e^{-\lambda H_{\bar{\theta}} \tau}\|_{op} \leq 1$. Also, by the relation between the operator norm and the Frobenius norm, we have

$$\|\nabla_{\theta} f_{\theta}(X) - \nabla_{\bar{\theta}} f_{\bar{\theta}}(X)\|_{op} \leq \|\nabla_{\theta} f_{\theta}(X) - \nabla_{\bar{\theta}} f_{\bar{\theta}}(X)\|_F \quad (47)$$

Besides, Lemma 1 of [25] indicates that there exists a $K_1 > 0$ such that for any X and $\theta, \bar{\theta} \in B(\theta_0, Cl^{-1/2})$,

$$\left\| \frac{1}{\sqrt{l}} \nabla_{\theta} f_{\theta}(X) - \frac{1}{\sqrt{l}} \nabla_{\bar{\theta}} f_{\bar{\theta}}(X) \right\|_F \leq K_1 \|\theta - \bar{\theta}\|_2 \quad (48)$$

Therefore, (47) gives

$$\|\nabla_{\theta} f_{\theta}(X) - \nabla_{\bar{\theta}} f_{\bar{\theta}}(X)\|_{op} \leq K_1 \sqrt{l} \|\theta - \bar{\theta}\|_2 \quad (49)$$

and then (45) is bounded as

$$\frac{1}{2} \|\nabla_{\theta} f_{\theta}(X) - \nabla_{\bar{\theta}} f_{\bar{\theta}}(X)\|_{op} (\|e^{-\lambda H_{\theta} \tau}\|_{op} + \|e^{-\lambda H_{\bar{\theta}} \tau}\|_{op}) \leq K_1 \sqrt{l} \|\theta - \bar{\theta}\|_2. \quad (50)$$

As for (46), notice that $\|\cdot\|_{op} \leq \|\cdot\|_F$ and (39) give us

$$\frac{1}{2} (\|\nabla_{\theta} f_{\theta}(X)\|_{op} + \|\nabla_{\bar{\theta}} f_{\bar{\theta}}(X)\|_{op}) \leq \sqrt{l} K_0. \quad (51)$$

Then, to bound $\|e^{-\lambda H_{\theta} \tau} - e^{-\lambda H_{\bar{\theta}} \tau}\|_{op}$ in (46), let us bound the following first

$$\begin{aligned} \|H_{\theta} - H_{\bar{\theta}}\|_F &= \left\| \frac{1}{l} \nabla_{\theta} f_{\theta}(X')^{\top} \nabla_{\theta} f_{\theta}(X') - \frac{1}{l} \nabla_{\bar{\theta}} f_{\bar{\theta}}(X')^{\top} \nabla_{\bar{\theta}} f_{\bar{\theta}}(X') \right\|_F \\ &= \frac{1}{l} \left\| \frac{1}{2} (\nabla_{\theta} f_{\theta}(X')^{\top} + \nabla_{\bar{\theta}} f_{\bar{\theta}}(X')^{\top}) (\nabla_{\theta} f_{\theta}(X') - \nabla_{\bar{\theta}} f_{\bar{\theta}}(X')) \right. \\ &\quad \left. + \frac{1}{2} (\nabla_{\theta} f_{\theta}(X')^{\top} - \nabla_{\bar{\theta}} f_{\bar{\theta}}(X')^{\top}) (\nabla_{\theta} f_{\theta}(X') + \nabla_{\bar{\theta}} f_{\bar{\theta}}(X')) \right\|_F \\ &\leq \frac{1}{l} \|\nabla_{\theta} f_{\theta}(X') + \nabla_{\bar{\theta}} f_{\bar{\theta}}(X')\|_F \|\nabla_{\theta} f_{\theta}(X') - \nabla_{\bar{\theta}} f_{\bar{\theta}}(X')\|_F \\ &\leq \frac{1}{l} (\|\nabla_{\theta} f_{\theta}(X')\|_F + \|\nabla_{\bar{\theta}} f_{\bar{\theta}}(X')\|_F) \|\nabla_{\theta} f_{\theta}(X') - \nabla_{\bar{\theta}} f_{\bar{\theta}}(X')\|_F \\ &\leq 2K_0 K_1 \|\theta - \bar{\theta}\|_2 \end{aligned} \quad (52)$$

Then, with the results above and a perturbation bound on matrix exponentials from [21], we have

$$\begin{aligned} \|e^{-\lambda H_{\theta} \tau} - e^{-\lambda H_{\bar{\theta}} \tau}\|_{op} &\leq \lambda \tau \|H_{\theta} - H_{\bar{\theta}}\|_{op} \cdot \exp(-\lambda \tau \cdot \min\{\sigma_{\min}(H_{\theta}), \sigma_{\min}(H_{\bar{\theta}})\}) \\ &\leq \lambda \tau \|H_{\theta} - H_{\bar{\theta}}\|_{op} \\ &\leq \lambda \tau \|H_{\theta} - H_{\bar{\theta}}\|_F \\ &\leq 2K_0 K_1 \lambda \tau \|\theta - \bar{\theta}\|_2 \end{aligned} \quad (53)$$

Hence, by (51) and (53), we can bound (46) as

$$\frac{1}{2} (\|\nabla_{\theta} f_{\theta}(X)\|_{op} + \|\nabla_{\bar{\theta}} f_{\bar{\theta}}(X)\|_{op}) \|e^{-\lambda H_{\theta}\tau} - e^{-\lambda H_{\bar{\theta}}\tau}\|_{op} \leq 2\sqrt{l} K_0^2 K_1 \lambda \tau \|\theta - \bar{\theta}\|_2 \quad (54)$$

Finally, with (50) and (54), we can bound (42) as

$$\|\nabla_{\theta} F((X, X', Y'), \theta) - \nabla_{\theta} F((X, X', Y'), \bar{\theta})\|_{op} \leq (K_1 + 2K_0^2 K_1 \lambda \tau) \sqrt{l} \|\theta - \bar{\theta}\|_2$$

Finally, combining these bounds on (45) and (46), we know that

$$\begin{aligned} \|J(\theta) - J(\bar{\theta})\|_F &= \left\| \frac{1}{\sqrt{l}} \nabla_{\theta} F((X, X', Y'), \theta) - \frac{1}{\sqrt{l}} \nabla_{\theta} F((X, X', Y'), \bar{\theta}) \right\|_F \\ &\leq \frac{\sqrt{kn}}{\sqrt{l}} \|\nabla_{\theta} F((X, X', Y'), \theta) - \nabla_{\theta} F((X, X', Y'), \bar{\theta})\|_{op} \\ &\leq \sqrt{kn} (K_1 + 2K_0^2 K_1 \lambda \tau) \|\theta - \bar{\theta}\|_2 \end{aligned} \quad (55)$$

Define $K_2 = \sqrt{kn} (K_1 + 2K_0^2 K_1 \lambda \tau)$, we have

$$\|J(\theta) - J(\bar{\theta})\|_F \leq K_2 \|\theta - \bar{\theta}\|_2 \quad (56)$$

Note that since $\tau = \mathcal{O}(\frac{1}{\lambda})$, we have $\lambda\tau = \mathcal{O}(1)$, indicating the factor $\lambda\tau$ is neglectable compared with other factors in K_2 . Hence, the various choices of τ under $\tau = \mathcal{O}(\frac{1}{\lambda})$ do not affect this proof.

Taking $K = \max\{K_0, K_2\}$ completes the proof. \square

B.2 Proof of Lemma 5

Proof of Lemma 5. It is known that $f_{\theta_0}(\cdot)$ converges in distribution to a mean zero Gaussian with the covariance \mathcal{K} determined by the parameter initialization [25]. As a result, for arbitrary $\delta_1 \in (0, 1)$ there exist constants $l_1 > 0$ and $R_1 > 0$, such that: $\forall l \geq l_1$, over random initialization, the following inequality holds true with probability at least $(1 - \delta_1)$,

$$\|f_{\theta_0}(X) - Y\|_2, \|f_{\theta_0}(X') - Y'\|_2 \leq R_1 \quad (57)$$

From (1), we know that $\forall (X, Y, X', Y') = \mathcal{T} \in D$,

$$F_{\theta_0}(X, X', Y') = f_{\theta'_0}(X)$$

where θ'_0 is the parameters after τ -step update on θ_0 over the meta-test task (X', Y') :

$$\begin{aligned} \theta_{\tau} &= \theta', \quad \theta_0 = \theta, \\ \theta_{i+1} &= \theta_i - \lambda \nabla_{\theta_i} \ell(f_{\theta_i}(X'), Y') \quad \forall i = 0, \dots, \tau - 1, \end{aligned} \quad (58)$$

Suppose the learning rate λ is sufficiently small, then based on Sec. (5), we have

$$F_{\theta_0}(X, X', Y') = f_{\theta_0}(X) + \hat{\Theta}_0(X, X') \hat{\Theta}_0^{-1} (I - e^{-\lambda \hat{\Theta}_0 \tau}) (f_{\theta_0}(X') - Y'). \quad (59)$$

where $\hat{\Theta}_0(\cdot, \star) = \nabla_{\theta_0} f_{\theta_0}(\cdot) \nabla_{\theta_0} f_{\theta_0}(\star)^{\top}$ and we use a shorthand $\hat{\Theta}_0 \equiv \hat{\Theta}_0(X', X')$.

[17] proves that for sufficiently large width, $\hat{\Theta}_0$ is positive definite and converges to Θ , the Neural Tangent Kernel, a full-rank kernel matrix with bounded positive eigenvalues. Let $\sigma_{\min}(\Theta)$ and $\sigma_{\max}(\Theta)$ denote the least and largest eigenvalue of Θ , respectively. Then, it is obvious that for a sufficiently over-parameterized neural network, the operator norm of $\hat{\Theta}(X, X') \hat{\Theta}^{-1} (I - e^{-\lambda \hat{\Theta} \tau})$ can be bounded based on $\sigma_{\min}(\Theta)$ and $\sigma_{\max}(\Theta)$. Besides, [3, 25] demonstrate that the neural net output at initialization, $f_{\theta_0}(\cdot)$, is a zero-mean Gaussian with small-scale covaraince. Combining these results and (57), we know there exists $R(R_1, N, \sigma_{\min}(\Theta), \sigma_{\max}(\Theta))$ such that

$$\|F_{\theta_0}(X, X', Y') - Y\|_2 \leq R(R_1, N, \sigma_{\min}(\Theta), \sigma_{\max}(\Theta)) \quad (60)$$

By taking an supremum over $R(R_1, N, \sigma_{\min}, \sigma_{\max})$ for each training task in $\{\mathcal{T}_i = (X_i, Y_i, X'_i, Y'_i)\}_{i \in [N]}$, we can get R_2 such that $\forall i \in [N]$

$$\|F_{\theta_0}(X_i, X'_i, Y'_i) - Y_i\|_2 \leq R_2 \quad (61)$$

and for $R_0 = \sqrt{N}R_2$, define δ_0 as some appropriate scaling of δ_1 , then the following holds true with probability $(1 - \delta_0)$ over random initialization,

$$\|g(\theta_0)\|_2 = \sqrt{\sum_{X,Y,X',Y' \in D} \|F((X, X', Y'), \theta_0) - y\|_2^2} \leq R_0 \quad (62)$$

□

B.3 Proof of Lemma 6

Proof of Lemma 6. The learning rate for meta-adaption, λ , is sufficiently small, so (2) becomes *continuous-time* gradient descent. Based on [25], for any task $\mathcal{T} = (X, Y, X', Y')$,

$$F_0(X, X', Y') = f_0(X) + \hat{\Theta}_0(X, X') \tilde{T}_{\hat{\Theta}_0}^\lambda(X', \tau) (Y' - f_0(X')), \quad (63)$$

where $\hat{\Theta}_0(\cdot, \star) = \frac{1}{l} \nabla_{\theta_0} f_0(\cdot) \nabla_{\theta_0} f_0(\star)^\top$, and $\tilde{T}_{\hat{\Theta}_0}^\lambda(\cdot, \tau) := \hat{\Theta}_0(\cdot, \cdot)^{-1} (I - e^{-\lambda \hat{\Theta}_0(\cdot, \cdot) \tau})$.

Then, we consider $\nabla_{\theta_0} F_0(X, X', Y')$, the gradient of $F_0(X, X', Y')$ in (63). Since [18] shows that the Hessian of any sufficiently wide neural network has almost zero operator norm, i.e. $\|\nabla_{\theta_0}^2 f_{\theta_0}(\cdot)\|_{\text{op}} \simeq 0$, we can drop the Hessian terms appearing in $\nabla_{\theta_0} F_0(X, X', Y')$, resulting in

$$\nabla_{\theta_0} F_0(X, X', Y') = \nabla_{\theta_0} f_0(X) - \hat{\Theta}_0(X, X') T_{\hat{\Theta}_0}^\lambda(X', \tau) \nabla_{\theta_0} f_0(X') \quad (64)$$

Since $\hat{\Phi}_0 \equiv \hat{\Phi}_0((\mathcal{X}, \mathcal{X}', \mathcal{Y}'), (\mathcal{X}, \mathcal{X}', \mathcal{Y}')) = \frac{1}{l} \nabla_{\theta_0} F_0(\mathcal{X}, \mathcal{X}', \mathcal{Y}') \nabla_{\theta_0} F_0(\mathcal{X}, \mathcal{X}', \mathcal{Y}')^\top$ and $F_0(\mathcal{X}, \mathcal{X}', \mathcal{Y}') = (F_0(X_i, X'_i, Y'_i))_{i=1}^N \in \mathbb{R}^{knN}$, we know $\hat{\Phi}_0$ is a block matrix with $N \times N$ blocks of size $kn \times kn$. For $i, j \in [N]$, the (i, j) -th block can be denoted as $[\hat{\Phi}_0]_{ij}$ such that

$$\begin{aligned} [\hat{\Phi}_0]_{ij} &= \frac{1}{l} \nabla_{\theta_0} F_0(X_i, X'_i, Y'_i) \nabla_{\theta_0} F_0(X_j, X'_j, Y'_j)^\top \\ &= \frac{1}{l} \nabla_{\theta_0} f_0(X_i) \nabla_{\theta_0} f_0(X_j)^\top \\ &\quad + \frac{1}{l} \hat{\Theta}_0(X_i, X'_i) \tilde{T}_{\hat{\Theta}_0}^\lambda(X'_i, \tau) \nabla_{\theta_0} f_0(X'_i) \nabla_{\theta_0} f_0(X'_j)^\top \tilde{T}_{\hat{\Theta}_0}^\lambda(X'_j, \tau)^\top \hat{\Theta}_0(X'_j, X_j) \\ &\quad - \frac{1}{l} \nabla_{\theta_0} f_0(X_i) \nabla_{\theta_0} f_0(X'_j)^\top \tilde{T}_{\hat{\Theta}_0}^\lambda(X'_j, \tau)^\top \hat{\Theta}_0(X'_j, X_j) \\ &\quad - \frac{1}{l} \hat{\Theta}_0(X_i, X'_i) \tilde{T}_{\hat{\Theta}_0}^\lambda(X'_i, \tau) \nabla_{\theta_0} f_0(X'_i) \nabla_{\theta_0} f_0(X_j)^\top \\ &= \hat{\Theta}_0(X_i, X_j) \\ &\quad + \hat{\Theta}_0(X_i, X'_i) \tilde{T}_{\hat{\Theta}_0}^\lambda(X'_i, \tau) \hat{\Theta}_0(X'_i, X'_j) \tilde{T}_{\hat{\Theta}_0}^\lambda(X'_j, \tau)^\top \hat{\Theta}_0(X'_j, X_j) \\ &\quad - \hat{\Theta}_0(X_i, X'_j) \tilde{T}_{\hat{\Theta}_0}^\lambda(X'_j, \tau)^\top \hat{\Theta}_0(X'_j, X_j) \\ &\quad - \hat{\Theta}_0(X_i, X'_i) \tilde{T}_{\hat{\Theta}_0}^\lambda(X'_i, \tau) \hat{\Theta}_0(X'_i, X_j) \end{aligned} \quad (65)$$

where we used the equivalences $\hat{\Theta}_0(\cdot, \star) = \hat{\Theta}_0(\star, \cdot)^\top$ and $\frac{1}{l} \nabla_{\theta_0} f_0(\cdot) \nabla_{\theta_0} f_0(\star) = \hat{\Theta}_0(\cdot, \star)$.

By Algebraic Limit Theorem for Functional Limits, we have

$$\begin{aligned}
& \lim_{l \rightarrow \infty} [\hat{\Phi}_0]_{ij} \\
&= \lim_{l \rightarrow \infty} \hat{\Theta}_0(X_i, X_j) \\
&+ \lim_{l \rightarrow \infty} \hat{\Theta}_0(X_i, X'_i) T_{\lim_{l \rightarrow \infty} \hat{\Theta}_0(X'_i, \tau)}^\lambda \lim_{l \rightarrow \infty} \hat{\Theta}_0(X'_i, X'_j) T_{\lim_{l \rightarrow \infty} \hat{\Theta}_0(X'_j, \tau)}^\lambda \lim_{l \rightarrow \infty} \hat{\Theta}_0(X'_j, X_j) \\
&- \lim_{l \rightarrow \infty} \hat{\Theta}_0(X_i, X'_j) T_{\lim_{l \rightarrow \infty} \hat{\Theta}_0(X'_j, \tau)}^\lambda \lim_{l \rightarrow \infty} \hat{\Theta}_0(X'_j, X_j) \\
&- \lim_{l \rightarrow \infty} \hat{\Theta}_0(X_i, X'_i) T_{\lim_{l \rightarrow \infty} \hat{\Theta}_0(X'_i, \tau)}^\lambda \hat{\Theta}_0(X'_i, X_j) \\
&= \Theta(X_i, X_j) \\
&+ \Theta(X_i, X'_i) \tilde{T}_{\hat{\Theta}}^\lambda(X'_i, \tau) \Theta(X'_i, X'_j) \tilde{T}_{\hat{\Theta}}^\lambda(X'_j, \tau)^\top \Theta(X'_j, X_j) \\
&- \Theta(X_i, X'_j) \tilde{T}_{\hat{\Theta}}^\lambda(X'_j, \tau)^\top \Theta(X'_j, X_j) \\
&- \Theta(X_i, X'_i) \tilde{T}_{\hat{\Theta}}^\lambda(X'_i, \tau) \Theta(X'_i, X_j)
\end{aligned} \tag{66}$$

where $\Theta(\cdot, \star) = \lim_{l \rightarrow \infty} \hat{\Theta}_0(\cdot, \star)$ is a deterministic kernel function, the Neural Tangent Kernel function (NTK) from the literature on supervised learning [17, 25, 3]. Specifically, $\hat{\Theta}_0(\cdot, \star)$ converges to $\Theta(\cdot, \star)$ in probability as the width l approaches infinity.

Hence, for any $i, j \in [N]$, as the width l approaches infinity, $[\hat{\Phi}_0]_{ij}$ converges in probability to a deterministic matrix $\lim_{l \rightarrow \infty} [\hat{\Phi}_0]_{ij}$, as shown by (66). Thus, the whole block matrix $\hat{\Phi}_0$ converges in probability to a deterministic matrix in the infinite width limit. Denote $\Phi = \lim_{l \rightarrow \infty} \hat{\Phi}_0$, then we know Φ is a deterministic matrix with each block expressed as (66).

Since $\hat{\Phi}_0 \equiv \hat{\Phi}_0((\mathcal{X}, \mathcal{X}', \mathcal{Y}), (\mathcal{X}, \mathcal{X}', \mathcal{Y})) = \frac{1}{l} \nabla_{\theta_0} F_0(\mathcal{X}, \mathcal{X}', \mathcal{Y}) \nabla_{\theta_0} F_0(\mathcal{X}, \mathcal{X}', \mathcal{Y})^\top$, it is a symmetric square matrix. Hence all eigenvalues of $\hat{\Phi}_0$ are greater or equal to 0, which also holds true for Φ . In addition, because of Assumption 5, Φ is positive definite, indicating $\sigma_{\min}(\Phi) > 0$. On the other hand, from [3], we know diagonal entries and eigenvalues of $\Theta(\cdot, \star)$ are positive real numbers upper bounded by $\mathcal{O}(L)$, as a direct result, it is easy to verify that the diagonal entries of the matrix Φ are also upper bounded, indicating $\sigma_{\max}(\Phi) < \infty$. Hence, we have $0 < \sigma_{\min}(\Phi) < \sigma_{\max}(\Phi) < \infty$.

Extension. It is easy to extend (66), the expression for $\Phi \equiv \lim_{l \rightarrow \infty} \hat{\Phi}_0((\mathcal{X}, \mathcal{X}', \mathcal{Y}), (\mathcal{X}, \mathcal{X}', \mathcal{Y}))$, to more general cases. Specifically, we can express $\Phi(\cdot, \star)$ analytically for arbitrary inputs. To achieve this, let us define a kernel function, $\phi : (\mathbb{R}^{n \times k} \times \mathbb{R}^{m \times k}) \times (\mathbb{R}^{n \times k} \times \mathbb{R}^{m \times k}) \mapsto \mathbb{R}^{nk \times nk}$ such that

$$\begin{aligned}
\phi((\cdot, \star), (\bullet, \star)) &= \Theta(\cdot, \bullet) + \Theta(\cdot, \star) \tilde{T}_{\hat{\Theta}}^\lambda(\star, \tau) \Theta(\star, \star) \tilde{T}_{\hat{\Theta}}^\lambda(\star, \tau)^\top \Theta(\star, \bullet) \\
&- \Theta(\cdot, \star) \tilde{T}_{\hat{\Theta}}^\lambda(\star, \tau) \Theta(\star, \bullet) - \Theta(\cdot, \star) \tilde{T}_{\hat{\Theta}}^\lambda(\star, \tau)^\top \Theta(\star, \bullet).
\end{aligned} \tag{67}$$

Then, it is obvious that for $i, j \in [N]$, the (i, j) -th block of Φ can be expressed as $[\Phi]_{ij} = \phi((X_i, X'_i), (X_j, X'_j))$.

For cases such as $\Phi((X, X'), (\mathcal{X}, \mathcal{X}')) \in \mathbb{R}^{kn \times knN}$, it is also obvious that $\Phi((X, X'), (\mathcal{X}, \mathcal{X}'))$ is a block matrix that consists of $1 \times N$ blocks of size $kn \times kn$, with the $(1, j)$ -th block as follows for $j \in [N]$,

$$[\Phi((X, X'), (\mathcal{X}, \mathcal{X}'))]_{1,j} = \phi((X, X'), (X_j, X'_j)).$$

□

B.4 Proof of Theorem 7

Proof of Theorem 7. Based on these lemmas presented above, we can prove Theorem 7.

Lemma 5 indicates that there exist R_0 and l^* such that for any width $l \geq l^*$, the following holds true over random initialization with probability at least $(1 - \delta_0/10)$,

$$\|g(\theta_0)\|_2 \leq R_0. \tag{68}$$

Consider $C = \frac{3KR_0}{\sigma}$ in Lemma 1.

First, we start with proving (30) and (33) by induction. Select $\tilde{l} > l^*$ such that (68) and (5) hold with probability at least $1 - \frac{\delta_0}{5}$ over random initialization for every $l \geq \tilde{l}$. As $t = 0$, by (29) and (5), we can easily verify that (30) and (33) hold true

$$\begin{cases} \|\theta_1 - \theta_0\|_2 &= \|\eta J(\theta_0)^\top g(\theta_0)\|_2 \leq \eta \|J(\theta_0)\|_{op} \|g(\theta_0)\|_2 \leq \frac{\eta_0}{l} \|J(\theta_0)\|_F \|g(\theta_0)\|_2 \leq \frac{K\eta_0}{\sqrt{l}} R_0. \\ \|g(\theta_0)\|_2 &\leq R_0 \end{cases}$$

Assume (30) and (33) hold true for any number of training step j such that $j < t$. Then, by (5) and (33), we have

$$\|\theta_{t+1} - \theta_t\|_2 \leq \eta \|J(\theta_t)\|_{op} \|g(\theta_t)\|_2 \leq \frac{K\eta_0}{\sqrt{l}} \left(1 - \frac{\eta_0\sigma_{\min}}{3}\right)^t R_0.$$

Beside, with the mean value theorem and (29), we have the following

$$\begin{aligned} \|g(\theta_{t+1})\|_2 &= \|g(\theta_{t+1} - \theta_t) + g(\theta_t)\|_2 \\ &= \|J(\theta_t^\mu)(\theta_{t+1} - \theta_t) + g(\theta_t)\|_2 \\ &= \|(I - \eta J(\theta_t^\mu)J(\theta_t)^\top)g(\theta_t)\|_2 \\ &\leq \|I - \eta J(\theta_t^\mu)J(\theta_t)^\top\|_{op} \|g(\theta_t)\|_2 \\ &\leq \|I - \eta J(\theta_t^\mu)J(\theta_t)^\top\|_{op} \left(1 - \frac{\eta_0\sigma_{\min}}{3}\right)^t R_0 \end{aligned}$$

where we define θ_t^μ as a linear interpolation between θ_t and θ_{t+1} such that $\theta_t^\mu := \mu\theta_t + (1 - \mu)\theta_{t+1}$ for some $0 < \mu < 1$.

Now, we will show that with probability $1 - \frac{\delta_0}{2}$,

$$\|I - \eta J(\theta_t^\mu)J(\theta_t)^\top\|_{op} \leq 1 - \frac{\eta_0\sigma_{\min}}{3}.$$

Recall that $\hat{\Phi}_0 \rightarrow \Phi$ in probability, proved by Lemma 6. Then, there exists \hat{l} such that the following holds with probability at least $1 - \frac{\delta_0}{5}$ for any width $l > \hat{l}$,

$$\|\Phi - \hat{\Phi}_0\|_F \leq \frac{\eta_0\sigma_{\min}}{3}.$$

Our assumption $\eta_0 < \frac{2}{\sigma_{\max} + \sigma_{\min}}$ makes sure that

$$\|I - \eta_0\Phi\|_{op} \leq 1 - \eta_0\sigma_{\min}.$$

Therefore, as $l \geq (\frac{18K^3R_0}{\sigma_{\min}^2})^2$, with probability at least $1 - \frac{\delta_0}{2}$ the following holds,

$$\begin{aligned} &\|I - \eta J(\theta_t^\mu)J(\theta_t)^\top\|_{op} \\ &= \|I - \eta_0\Phi + \eta_0\Phi - \hat{\Phi}_0 + \eta(J(\theta_0)J(\theta_0)^\top - J(\theta_t^\mu)J(\theta_t)^\top)\|_{op} \\ &\leq \|I - \eta_0\Phi\|_{op} + \eta_0\|\Phi - \hat{\Phi}_0\|_{op} + \eta\|J(\theta_0)J(\theta_0)^\top - J(\theta_t^\mu)J(\theta_t)^\top\|_{op} \\ &\leq 1 - \eta_0\sigma_{\min} + \frac{\eta_0\sigma_{\min}}{3} + \eta_0K^2(\|\theta_t - \theta_0\|_2 + \|\theta_t^\mu - \theta_0\|_2) \\ &\leq 1 - \eta_0\sigma_{\min} + \frac{\eta_0\sigma_{\min}}{3} + \frac{6\eta_0K^3R_0}{\sigma_{\min}\sqrt{l}} \\ &\leq 1 - \frac{\eta_0\sigma_{\min}}{3} \end{aligned}$$

where we used the equality $\frac{1}{l}J(\theta_0)J(\theta_0)^\top = \hat{\Phi}_0$.

Hence, as we choose $\Lambda = \max\{l^*, \tilde{l}, \hat{l}, (\frac{18K^3R_0}{\sigma_{\min}^2})^2\}$, the following holds for any width $l > \Lambda$ with probability at least $1 - \delta_0$ over random initialization

$$\|g(\theta_{t+1})\|_2 \leq \|I - \eta J(\theta_t^\mu)J(\theta_t)^\top\|_{op} \left(1 - \frac{\eta_0\sigma_{\min}}{3}\right)^t R_0 \leq \left(1 - \frac{\eta_0\sigma_{\min}}{3}\right)^{t+1} R_0, \quad (69)$$

which finishes the proof (33).

Finally, we prove (31) by

$$\begin{aligned}
\|\hat{\Phi}_0 - \hat{\Phi}_t\|_F &= \frac{1}{l} \|J(\theta_0)J(\theta_0)^\top - J(\theta_t)J(\theta_t)^\top\|_F \\
&\leq \frac{1}{l} \|J(\theta_0)\|_{op} \|J(\theta_0)^\top - J(\theta_t)^\top\|_F + \frac{1}{l} \|J(\theta_t) - J(\theta_0)\|_{op} \|J(\theta_t)^\top\|_F \\
&\leq 2K^2 \|\theta_0 - \theta_t\|_2 \\
&\leq \frac{6K^3 R_0}{\sigma_{\min} \sqrt{l}},
\end{aligned}$$

where we used (30) and Lemma 1. \square

C Proof of Corollary 2.1 (GBML Output)

In this section, we will provide proof of Corollary 2.1. Briefly speaking, with the help of Theorem 7, we first show the training dynamics of GBML with over-parameterized DNNs can be described by a differential equation, which is analytically solvable. By solving this differential equation, we obtain the expression for GBML output on any training or test task.

Below, we first restate Corollary 2.1, and then provide the proof.

Corollary 7.1 (GBML Output (Corollary 2.1 Restated)). *In the setting of Theorem 2, the training dynamics of the GBML can be described by a differential equation*

$$\frac{dF_t(\mathcal{X}, \mathcal{X}', \mathcal{Y}')}{dt} = -\eta \hat{\Phi}_0(F_t(\mathcal{X}, \mathcal{X}', \mathcal{Y}') - \mathcal{Y})$$

where we denote $F_t \equiv F_{\theta_t}$ and $\hat{\Phi}_0 \equiv \hat{\Phi}_{\theta_0}((\mathcal{X}, \mathcal{X}', \mathcal{Y}'), (\mathcal{X}, \mathcal{X}', \mathcal{Y}'))$ for convenience.

Solving this differential equation, we obtain the meta-output of GBML on training tasks at any training time as

$$F_t(\mathcal{X}, \mathcal{X}', \mathcal{Y}') = (I - e^{-\eta \hat{\Phi}_0 t})\mathcal{Y} + e^{-\eta \hat{\Phi}_0 t} F_0(\mathcal{X}, \mathcal{X}', \mathcal{Y}'). \quad (70)$$

Similarly, on arbitrary test task $\mathcal{T} = (X, Y, X', Y')$, the meta-output of GBML is

$$F_t(X, X', Y') = F_0(X, X', Y') + \hat{\Phi}_0(X, X', Y') T_{\hat{\Phi}_0}^\eta(t) (\mathcal{Y} - F_0(\mathcal{X}, \mathcal{X}', \mathcal{Y}')) \quad (71)$$

where $\hat{\Phi}_0(\cdot) \equiv \hat{\Phi}_{\theta_0}(\cdot, (\mathcal{X}, \mathcal{X}', \mathcal{Y}'))$ and $T_{\hat{\Phi}_0}^\eta(t) = \hat{\Phi}_0^{-1} (I - e^{-\eta \hat{\Phi}_0 t})$ are shorthand notations.

Proof. For the optimization of GBML, the gradient descent on θ_t with learning rate η can be expressed as

$$\begin{aligned}
\theta_{t+1} &= \theta_t - \eta \nabla_{\theta_t} \mathcal{L}(\theta_t) \\
&= \theta_t - \frac{1}{2} \eta \nabla_{\theta_t} \|F_{\theta_t}(\mathcal{X}, \mathcal{X}', \mathcal{Y}') - \mathcal{Y}\|_2^2 \\
&= \theta_t - \eta \nabla_{\theta_t} F_{\theta_t}(\mathcal{X}, \mathcal{X}', \mathcal{Y}')^\top (F_{\theta_t}(\mathcal{X}, \mathcal{X}', \mathcal{Y}') - \mathcal{Y})
\end{aligned} \quad (72)$$

Since the learning rate η is sufficiently small, the *discrete-time* gradient descent above can be re-written in the form of *continuous-time* gradient descent (i.e., gradient flow),

$$\frac{d\theta_t}{dt} = -\eta \nabla_{\theta_t} F_{\theta_t}(\mathcal{X}, \mathcal{X}', \mathcal{Y}')^\top (F_{\theta_t}(\mathcal{X}, \mathcal{X}', \mathcal{Y}') - \mathcal{Y})$$

Then, the training dynamics of the meta-output $F_t(\cdot) \equiv F_{\theta_t}(\cdot)$ can be described by the following differential equation,

$$\begin{aligned}
\frac{dF_t(\mathcal{X}, \mathcal{X}', \mathcal{Y}')}{dt} &= \nabla_{\theta_t} F_t(\mathcal{X}, \mathcal{X}', \mathcal{Y}') \frac{d\theta_t}{dt} \\
&= -\eta \nabla_{\theta_t} F_t(\mathcal{X}, \mathcal{X}', \mathcal{Y}') \nabla_{\theta_t} F_t(\mathcal{X}, \mathcal{X}', \mathcal{Y}')^\top (F_t(\mathcal{X}, \mathcal{X}', \mathcal{Y}') - \mathcal{Y}) \\
&= -\eta \hat{\Phi}_t (F_t(\mathcal{X}, \mathcal{X}', \mathcal{Y}') - \mathcal{Y})
\end{aligned} \quad (73)$$

where $\hat{\Phi}_t = \hat{\Phi}_t((\mathcal{X}, \mathcal{X}', \mathcal{Y}'), (\mathcal{X}, \mathcal{X}', \mathcal{Y}')) = \nabla_{\theta_t} F_t(\mathcal{X}, \mathcal{X}', \mathcal{Y}') \nabla_{\theta_t} F_t(\mathcal{X}, \mathcal{X}', \mathcal{Y}')^\top$.

On the other hand, Theorem 7 gives the following bound in (31),

$$\sup_t \|\hat{\Phi}_0 - \hat{\Phi}_t\|_F \leq \frac{6K^3 R_0}{\sigma_{\min}} l^{-\frac{1}{2}}, \quad (74)$$

indicating $\hat{\Phi}_t$ stays almost constant during training for sufficiently over-parameterized neural networks (i.e., large enough width l). Therefore, we can replace $\hat{\Phi}_t$ by $\hat{\Phi}_0$ in (73), and get

$$\frac{dF_t(\mathcal{X}, \mathcal{X}', \mathcal{Y}')}{dt} = -\eta \hat{\Phi}_0 (F_t(\mathcal{X}, \mathcal{X}', \mathcal{Y}') - \mathcal{Y}), \quad (75)$$

which is an ordinary differential equation (ODE) for the meta-output $F_t(\mathcal{X}, \mathcal{X}', \mathcal{Y}')$ w.r.t. the training time t .

This ODE is analytically solvable with a unique solution. Solving it, we obtain the meta-output on training tasks at any training time t as,

$$F_t(\mathcal{X}, \mathcal{X}', \mathcal{Y}') = (I - e^{-\eta \hat{\Phi}_0 t}) \mathcal{Y} + e^{-\eta \hat{\Phi}_0 t} F_0(\mathcal{X}, \mathcal{X}', \mathcal{Y}'). \quad (76)$$

The solution can be easily extended to any test task $\mathcal{T} = (X, Y, X', Y')$, and the meta-output on the test task at any training time is

$$F_t(X, X', Y') = F_0(X, X', Y') + \hat{\Phi}_0(X, X', Y') T_{\hat{\Phi}_0}^\eta(t) (\mathcal{Y} - F_0(\mathcal{X}, \mathcal{X}', \mathcal{Y}')), \quad (77)$$

where $\hat{\Phi}_0(\cdot) \equiv \hat{\Phi}_{\theta_0}(\cdot, (\mathcal{X}, \mathcal{X}', \mathcal{Y}'))$ and $T_{\hat{\Phi}_0}^\eta(t) = \hat{\Phi}_0^{-1} (I - e^{-\eta \hat{\Phi}_0 t})$ are shorthand notations. \square

D Introduction to Kernel Regression

The purpose of this section is to familiarize readers with kernel regression, a well-studied method with theoretical guarantees for regression and classification in the setting of supervised learning.

Consider a supervised learning task of binary classification, $\mathcal{T}(X, Y, X', Y') \in \mathbb{R}^{d \times n} \times \mathbb{R}^n \times \mathbb{R}^{d \times m} \times \mathbb{R}^m$, where (X', Y') is the training dataset and (X, Y) is the test dataset. Suppose we have kernel function $\Psi(\cdot, \star)$, then the prediction of a standard kernel regression on test samples is

$$\hat{Y} = \Psi(X, X') \Psi(X', X')^{-1} Y' \quad (78)$$

where $\Psi(X, X') \in \mathbb{R}^{n \times m}$ and $\Psi(X', X') \in \mathbb{R}^{m \times m}$.

Since it is binary classification, the set of training labels, Y' , is usually a vector with elements as $\{0, 1\}$ (or $\{-1, 1\}$), where 0 and 1 represent two classes, separately. In this case, for an element of \hat{Y} , if its value is greater or equal than $\frac{1}{2}$, then it is considered to predict the class of 1; if its value is less than $\frac{1}{2}$, then it predicts the class of 0.

In the case of multi-class classification, kernel regression methods usually use one-hot labels. For instance, if there are 5 classes and the training labels are $[3, 2, 5, 3, \dots]$, then the one-hot version of Y' is expressed as

$$Y' = \begin{bmatrix} 0 & 0 & 1 & 0 & 0 \\ 0 & 1 & 0 & 0 & 0 \\ 0 & 0 & 0 & 0 & 1 \\ 0 & 0 & 1 & 0 & 0 \\ \vdots & \vdots & \vdots & \vdots & \vdots \end{bmatrix} \quad (79)$$

In this way, each column represents an individual dimension. Specifically, the kernel regression, (78), is doing regression in each of these dimensions separately.

The derived kernel regression for few-shot learning in Theorem 3 is very different from this standard one, but the forms are similar.

E Gradient-Based Meta-Learning as Kernel Regression

In this section, we first make an assumption on the scale of parameter initialization, then we restate Theorem 3. After that, we provide the proof for Theorem 3.

[25] shows the output of a neural network randomly initialized following (15) is a zero-mean Gaussian with covariance determined by σ_w and σ_b , the variances corresponding to the initialization of weights and biases. Hence, small values of σ_w and σ_b can make the outputs of randomly initialized neural networks approximately zero. We adopt the following assumption from [3] to simplify the expression of the kernel regression in Theorem 3.

Assumption 6 (Small Scale of Parameter Initialization). *The scale of parameter initialization is sufficiently small, i.e., σ_w, σ_b in (15) are small enough, so that $f_0(\cdot) \simeq 0$.*

Note the goal of this assumption is to make the output of the randomly initialized neural network negligible. The assumption is quite common and mild, since, in general, the outputs of randomly initialized neural networks are of small scale compared with the outputs of trained networks [25].

Theorem 8 (GBML as Kernel Regression (Theorem 3 Restated)). *Suppose learning rates η and λ are infinitesimal. As the network width l approaches infinity, with high probability over random initialization of the neural net, the GBML output, (9), converges to a special kernel regression,*

$$F_t(X, X', Y') = G_\Theta^\tau(X, X', Y') + \Phi((X, X'), (\mathcal{X}, \mathcal{X}')) T_\Phi^\eta(t) (\mathcal{Y} - G_\Theta^\tau(\mathcal{X}, \mathcal{X}', \mathcal{Y}')) \quad (80)$$

where G is a function defined below, Θ is the neural tangent kernel (NTK) function from [17] that can be analytically calculated without constructing any neural net, and Φ is a new kernel, which name as Meta Neural Kernel (MNK). The expression for G is

$$G_\Theta^\tau(X, X', Y') = \Theta(X, X') \tilde{T}_\Theta^\lambda(X', \tau) Y'. \quad (81)$$

where $\tilde{T}_\Theta^\lambda(\cdot, \tau) := \Theta(\cdot, \cdot)^{-1} (I - e^{-\lambda \Theta(\cdot, \cdot) \tau})$. Besides, $G_\Theta^\tau(\mathcal{X}, \mathcal{X}', \mathcal{Y}') = (G_\Theta^\tau(X_i, X'_i, Y'_i))_{i=1}^N$.

The MNK is defined as $\Phi \equiv \Phi((\mathcal{X}, \mathcal{X}'), (\mathcal{X}, \mathcal{X}')) \in \mathbb{R}^{knN \times knN}$, which is a block matrix that consists of $N \times N$ blocks of size $kn \times kn$. For $i, j \in [N]$, the (i, j) -th block of Φ is

$$[\Phi]_{ij} = \phi((X_i, X'_i), (X_j, X'_j)) \in \mathbb{R}^{kn \times kn}, \quad (82)$$

where $\phi : (\mathbb{R}^{n \times k} \times \mathbb{R}^{m \times k}) \times (\mathbb{R}^{n \times k} \times \mathbb{R}^{m \times k}) \rightarrow \mathbb{R}^{kn \times kn}$ is a kernel function defined as

$$\begin{aligned} \phi((\cdot, \star), (\bullet, \star)) &= \Theta(\cdot, \bullet) + \Theta(\cdot, \star) \tilde{T}_\Theta^\lambda(\star, \tau) \Theta(\star, \star) \tilde{T}_\Theta^\lambda(\star, \tau)^\top \Theta(\star, \bullet) \\ &\quad - \Theta(\cdot, \star) \tilde{T}_\Theta^\lambda(\star, \tau) \Theta(\star, \bullet) - \Theta(\cdot, \star) \tilde{T}_\Theta^\lambda(\star, \tau)^\top \Theta(\star, \bullet). \end{aligned} \quad (83)$$

The $\Phi((X, X'), (\mathcal{X}, \mathcal{X}')) \in \mathbb{R}^{kn \times knN}$ in (11) is also a block matrix, which consists of $1 \times N$ blocks of size $kn \times kn$, with the $(1, j)$ -th block as follows for $j \in [N]$,

$$[\Phi((X, X'), (\mathcal{X}, \mathcal{X}'))]_{1,j} = \phi((X, X'), (X_j, X'_j)). \quad (84)$$

Proof. First, (9) shows that the output of GBML on any test task $\mathcal{T} = (X, Y, X', Y')$ can be expressed as

$$F_t(X, X', Y') = F_0(X, X', Y') + \hat{\Phi}_0(X, X', Y') T_{\hat{\Phi}_0}^\eta(t) (\mathcal{Y} - F_0(\mathcal{X}, \mathcal{X}', \mathcal{Y}')) \quad (85)$$

Note (63) in Appendix B.3 shows that

$$F_0(X, X', Y') = f_0(X) + \hat{\Theta}_0(X, X') \tilde{T}_{\hat{\Theta}_0}^\lambda(X', \tau) (Y' - f_0(X')), \quad (86)$$

With Assumption 6, we can drop the terms $f_0(X)$ and $f_0(X')$ in (86). Besides, from [17, 3, 25], we know $\lim_{l \rightarrow \infty} \hat{\Theta}_0(\cdot, \star) = \Theta(\cdot, \star)$, the Neural Tangent Kernel (NTK) function, a deterministic kernel function. Therefore, $F_0(X, X', Y')$ can be described by the following function as the width approaches infinity,

$$\lim_{l \rightarrow \infty} F_0(X, X', Y') = G_\Theta^\tau(X, X', Y') = \Theta(X, X') \tilde{T}_\Theta^\lambda(X', \tau) Y'. \quad (87)$$

where $\tilde{T}_\Theta^\lambda(\cdot, \tau) := \Theta(\cdot, \cdot)^{-1} (I - e^{-\lambda \Theta(\cdot, \cdot) \tau})$. Besides, $G_\Theta^\tau(\mathcal{X}, \mathcal{X}', \mathcal{Y}') = (G_\Theta^\tau(X_i, X'_i, Y'_i))_{i=1}^N$.

In addition, from Lemma 6, we know $\lim_{l \rightarrow \infty} \hat{\Phi}_0(\cdot, \star) = \Phi(\cdot, \star)$. Combined this with (87), we can express (85) in the infinite width limit as

$$F_t(X, X', Y') = G_\Theta^\tau(X, X', Y') + \Phi((X, X'), (\mathcal{X}, \mathcal{X}')) T_\Phi^\eta(t) (\mathcal{Y} - G_\Theta^\tau(\mathcal{X}, \mathcal{X}', \mathcal{Y}')) \quad (88)$$

where $\Phi(\cdot, \star)$ is a kernel function that we name as Meta Neural Kernel function. The derivation of its expression shown in (82)-(84) can be found in Appendix B.3. \square

F Experiments of MNK vs. GBML on Few-Shot Classification

F.1 Implementation Details

Implementation of MNK. As discussed in Sec. 5, the Meta Neural Kernel Φ is a composite kernel built upon a base kernel function, Θ , which is precisely the Neural Tangent Kernel (NTK) derived in supervised learning [17, 25, 3]. Since we consider the few-shot image classification problem, we need a base kernel function that suits the image domain. Hence, we adopt Convolutional Neural Tangent Kernel (CNTK) [3], the NTK derived from over-parameterized Convolution Neural Networks (CNNs), as the base kernel function. Since the official CNTK code¹⁰ is written in CUDA with a Python interface, it needs NVIDIA GPU for computation. Therefore, we use a workstation with 4 GPUs of RTX 2080 ti. Besides, we implement MNK in Python. The total computation cost for our conducted experiment of MNK on Omniglot is about 1000 GPU hours on this workstation. Specifically, we first compute all CNTK values that are used for MNK experiments, which take nearly 1000 GPU hours. Then we perform experiments on MNK with these pre-computed CNTK values.

Implementation of MAML and iMAML. As for the implementation of MAML, we use the code from [15], which obtain similar or better performance than the original MAML paper [11]. The details of neural network construction and learning rate can be found in [15] or its public codebase at <https://github.com/facebookresearch/higher/blob/master/examples/maml-omniglot.py>. We also use the data loader for the Omniglot dataset in [15]. For a fair comparison, we adopt a PyTorch implementation¹¹ of iMAML [38] built upon the codebase of [15].

Why there is No Experiment on Mini-ImageNet. For few-shot learning, there are two most popular benchmark, the Omniglot dataset [24] and Mini-ImageNet dataset [42]¹². Samples in the Omniglot dataset are greyscaled images of size 28×28 , while samples in the Mini-ImageNet dataset are RGB images of size 84×84 . As a result, for two training sets of the same sample size in the two datasets, respectively, the computation cost of the Mini-ImageNet one is **81 times** as the Omniglot one. The reason behind this is that the MNK computation is quadratic in the size of each sample, d , since the base kernels (i.e., CNTK [3] in our implementation) have $\mathcal{O}(d^2)$ computation cost. The dimension of a Mini-ImageNet sample is $84 \times 84 \times 3$, and the dimension of an Omniglot sample is $28 \times 28 \times 1$. Although during the computation of NTK or MNK, these image samples are not flattened into $1-d$ vectors, we can consider them as flattened $1-d$ vectors to calculate the computation cost without loss of generality (see [3, 4, 28] for computation cost of NTK). Hence, it is easy to get the “81 times” result by $\left(\frac{84 \times 3}{28 \times 1}\right)^2 = 81$. Note that our experiments on Omniglot are already constrained to small-data cases due to the high computation cost and our limited computation resource. For Mini-ImageNet, the scale of our experiments has to be 81 times smaller, which is not meaningful or interesting in practice. That is why we do not conduct experiments on the Mini-ImageNet dataset.

Why Digital or One-Hot Labels cannot be Directly Used. In Sec. 6, we briefly discussed why digital or one-hot labels could not be directly used for kernel regression on few-shot classification. Here, we explain the reasons more detailedly. In general, digital labels are not suitable for regression methods, since regression methods are usually based on ℓ_2 loss that is not designed for categorical labels. Hence, in the application of kernel regression on multi-class classification, the one-hot encoding of digital labels is the most used label preprocessing technique¹³. Even though one-hot label encoding works for kernel regression on multi-class classification, a problem of supervised learning, it does not fit the few-shot multi-class classification, which contains multiple supervised learning tasks. We can see the issue easily by a thought experiment: interchangeable labels. In the case of standard kernel regression for multi-class classification, a supervised learning task, the labels for different classes can be interchanged without causing any influence on the final prediction of the model, which can be well explained by the example of (79). In that example, there are five classes, and the digital labels for training samples are $[3, 2, 5, 3, \dots]$, then the corresponding one-hot encoded

¹⁰<https://github.com/ruosongwang/CNTK>

¹¹<https://github.com/prolearner/hypertorch>

¹²The Mini-Imagenet is proposed in [42]. For practical use of the dataset, please use the following tool to generate this dataset from the ImageNet dataset [7]: <https://github.com/yaoyao-liu/mini-imagenet-tools>

¹³For instance, this is what scikit-learn [36], one of the most popular code package for machine learning, uses for kernel methods: <https://scikit-learn.org/stable/modules/preprocessing.html#preprocessing-categorical-features>.

labels, Y' , is expressed as

$$Y' = \begin{bmatrix} 0 & 0 & 1 & 0 & 0 \\ 0 & 1 & 0 & 0 & 0 \\ 0 & 0 & 0 & 0 & 1 \\ 0 & 0 & 1 & 0 & 0 \\ \vdots & \vdots & \vdots & \vdots & \vdots \end{bmatrix} \quad (89)$$

If we interchange two of these digital labels, e.g., $3 \leftrightarrow 5$, then the third and fifth columns of Y' are interchanged. However, this operation has no impact on the kernel regression model, (78), since the prediction of the model, \hat{Y} , also interchanges its third and fifth columns correspondingly. Finally, the prediction of the class of each sample remains the same.

However, in the setting of few-shot multi-class classification, this label interchangeability does not hold. For simplicity, consider a few-shot multi-class classification problem with only two training tasks, $\mathcal{T}_1 = (X_1, Y_1, X'_1, Y'_1)$ and $\mathcal{T}_2 = (X_2, Y_2, X'_2, Y'_2)$. Suppose each task contains five unique classes of samples. If we continue using one-hot labels, the classes for samples in \mathcal{T}_1 and \mathcal{T}_2 are labelled by the one-hot encoding of $\{1, 2, 3, 4, 5\}$. Assume Y_1 is the same as the Y' in (89), and Y_2 is the one-hot version of digital labels $\{1, 5, 2, 3, \dots\}$. Then, the labels for query samples in training tasks, i.e., \mathcal{Y} in (11), can be seen as a concatenation of Y_1 and Y_2 :

$$\mathcal{Y} = \begin{bmatrix} 0 & 0 & \mathbf{1} & 0 & \mathbf{0} \\ 0 & 1 & \mathbf{0} & 0 & \mathbf{0} \\ 0 & 0 & \mathbf{0} & 0 & \mathbf{1} \\ 0 & 0 & \mathbf{1} & 0 & \mathbf{0} \\ \vdots & \vdots & \vdots & \vdots & \vdots \\ 1 & 0 & 0 & 0 & 0 \\ 0 & 0 & 0 & 0 & 1 \\ 0 & 1 & 0 & 0 & 0 \\ 0 & 0 & 1 & 0 & 0 \\ \vdots & \vdots & \vdots & \vdots & \vdots \end{bmatrix} \quad (90)$$

where the upper rows represent Y_1 and the lower rows with the italic font are Y_2 .

Since kernel regression treats each column as an individual dimension, different columns do not affect each other. However, elements in the same column have a correlation with each other, since they are in the same dimension. Therefore, labels for different classes cannot be interchanged in the example of (90). For instance, if we interchange the two digital labels, $3 \leftrightarrow 5$, for \mathcal{T}_1 , then the bold elements in Y_1 are interchanged between the third and fifth columns. However, the elements in the third column of Y_1 have a correlation with the elements of Y_2 in the third column. Thus the label change affects the prediction of the samples corresponding to the third column. Similarly, the fifth column is also impacted. Hence, interchanging digital labels of classes in a single task has an effect on the prediction of the kernel regression—the prediction of the kernel regression does not remain invariant w.r.t. interchanged labels. *That is why the label inter-changeability is broken for few-shot multi-class classification, which should not happen, since the labels for classes in each task are assigned in an artificial and arbitrary order. As a result, the one-hot encoding of labels is ill-defined for kernel regression on few-shot multi-class classification problems. Therefore, we need to find a new label encoding method without the problem of broken label interchangeability.*

A New Label Preprocessing/Encoding Method. To resolve the problem about labels stated above, we propose a new label encoding method without the issue of broken label interchangeability. Briefly, we expect the encoded labels to be invariant w.r.t. any choice of digital labels (e.g., $\{1, 2, 3, 4, 5\}$) assigned to different classes. To achieve this, we design a label encoding/preprocessing technique that projects digital labels from different tasks into a single vector space. Specifically, we first choose a fixed feature extractor ψ such that it can transform any sample x into a feature vector, $\psi(x) \in \mathbb{R}^h$, in a h -d Euclidean space. Then, we use this feature extractor to convert all samples in each training task into feature vectors. For test tasks, we do this for support samples only. After that, in each task, we compute the centroids of feature vectors corresponding to samples in each class (i.e., obtain five centroids for the five classes in each task), and use the centroid (i.e., a h -d vector) of each class as its new label. In this way, classes from various tasks are marked by different vector labels, and digital

label are interchanged here (e.g., $3 \leftrightarrow 5$) without any effect on the kernel regression prediction, since these encoded labels for classes are solely determined by the samples in the classes and do not depend on the assignment of digital labels.

Feature Extractor. We train a randomly initialized convolutional neural net (CNN) over all training data $(\mathcal{X}, \mathcal{Y}, \mathcal{X}', \mathcal{Y}')$ in the *supervised learning* way, then take its hidden layers (i.e., the CNN with the last layer removed) as the fixed feature extractor used in the label encoding explained above. However, we notice that this feature extractor performs poorly in the extremely small-data case, i.e., the case of # Characters = 5 in Table 1, due to the well-known over-fitting of neural nets to small-scale datasets. Hence, inspired by [6], we directly use a randomly initialized CNN without any training as the feature extractor in the case of # Characters = 5. For the implementation of the CNN, we directly adopt the demo code¹⁴ from [15], which constructs a CNN with three convolutional layers with max pooling, followed by a fully connected output layer. For trained CNNs as feature extractors, we take the number of channels as 250; for randomly initialized CNNs as feature extractors, we use 1000 channels instead.

Hyperparameters. For MAML and iMAML, we adopt the original hyper-parameters in their implementations¹⁵. For the implementation of the MNK method shown in Theorem 3, we adopt $\tau = \infty$ and $t = \infty$, which simply leads to vanishing exponential terms¹⁶ in (11). Also, we adopt the commonly used ridge regularization for kernel regression¹⁷, with coefficient as 10^{-5} , to stabilize the kernel regression computation.

Ablation Study on the Label Preprocessing/Encoding Method. One might be curious if the gains obtained by MNK over MAML and iMAML are because of some additional information provided by the label encoding operation described above. To address this concern, we perform an ablation study on MAML to compare its performance with the original *digital labels* and the *encoded labels*. Notice that with the digital labels, MAML uses the cross-entropy loss function following its original implementation [11]. In contrast, the cross-entropy loss function is ill-defined for encoded labels since they are not integers. Thus, we adopt the l_2 loss function in the case of encoded labels. For a fair comparison, we perform the identical label encoding operation used by our implementation of MNK, and provide the encoded labels to MAML. The empirical results are summarized in Table 2. We can see that MAML with label encoding performs poorly in the extreme small-data cases (i.e., # Characters = 5, 10), and can obtain performance close to MAML with original labels as the data size becomes relatively larger. However, the performance of MAML with encoded labels is always lower than MAML with original labels. Hence, we can conclude that the additional information provided in the encoded labels should not be the key to the success of MNK. (We do not perform the ablation study on iMAML [38], since iMAML adds some strong regularization terms to its cross-entropy losses, and changing the loss function from the cross-entropy to the l_2 one may have a negative effect on the regularization, which is key to iMAML.)

# Characters	5	10	20	40	80
% of Omniglot	0.42%	0.83%	1.67%	3.33%	6.67%
MAML (Original)	78.7 \pm 2.1	83.2 \pm 1.3	85.9 \pm 1.1	88.3 \pm 0.7	90.9 \pm 0.6
MAML (Label Encoding)	46.8 \pm 2.1	72.8 \pm 1.9	83.3 \pm 1.0	87.4 \pm 0.7	89.8 \pm 0.5

Table 2: An ablation study on the label encoding. The setting is the same as the setting of Table 1.

¹⁴<https://github.com/facebookresearch/higher/blob/master/examples/maml-omniglot.py>

¹⁵<https://github.com/facebookresearch/higher/blob/master/examples/maml-omniglot.py> and <https://github.com/prolearner/hypertorch>

¹⁶This choice is also used in [3, 4, 28]

¹⁷Same as the ridge regularization for kernel regression used in scikit-learn [36]: https://scikit-learn.org/stable/modules/kernel_ridge.html